SeaKeeping (SK)

Validation Studies

Contents: **Page**

2D Hydrodynamic Coefficients for Simple Shapes..... 2

Box Section..... 3

Triangle Section..... 5

Cylindrical Section..... 7

3D Forces and Phase Angles at Multiple Headings for Simple Barge Geometries..... 8

3D Forces and Phase Angles at Multiple Headings for a Tanker Hull 17

Absolute and Relative RAOs and Accelerations for the Flokstra Containership..... 25

RAOs for KCS with Weight Distribution in Head Seas and Zero Speed 43

References and Additional Resources..... 45

2D Hydrodynamic Coefficients for Simple Shapes

The most fundamental computation performed by SeaKeeping is the solution of the two-dimensional radiation problem for each section. The solution leads to the two-dimensional hydrodynamic added mass and damping coefficients, and the two-dimensional complex diffraction forcing amplitude for the section. In this validation study, these two-dimensional results are compared to model test data published by Vugts (1968).

Three different geometries were analyzed: a box section, a triangular section, and a cylindrical section, as shown by Figure 1. For the box, three beam-to-draft (B/T) ratios were also analyzed. The beam factor (see SK User's Manual) was taken at the default value of 8 for all box shaped sections, and 32 for the triangular and cylindrical sections. The resulting non-dimensional coefficients, and the total heave, sway, and roll forcing amplitudes are given by Figure 2 through Figure 17. In most cases, fair to good agreement between the experimental data and the computational result is obtained. Appreciable differences, such as the case in roll for the triangular and cylindrical section, are attributable to neglecting viscosity, flow-separation, and other significant nonlinearities evident in the real-world flow. Further deviation is observed in the cylindrical section in roll and sway-into-roll. Here, theoretical results are practically zero, as viscous effects account for most of the experimental observations. **These assumptions are typical of two-dimensional potential flow based solvers, such as the one used by SeaKeeping, and the deviations are expected.**

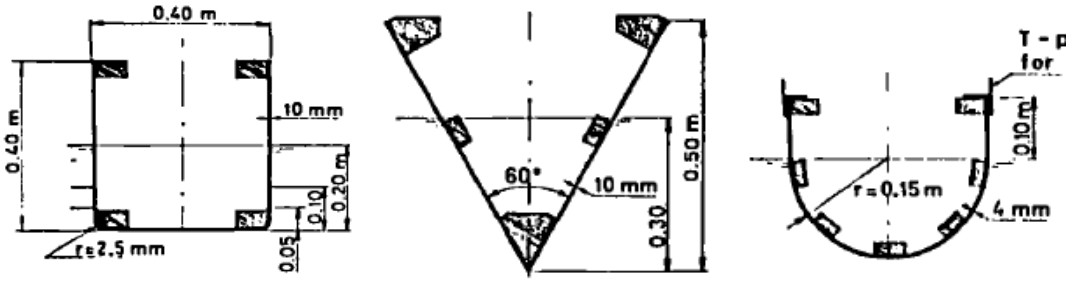

Figure 1. Vugts' Two-Dimensional Section Geometries

In the case of roll for the box section at B/T = 4 and B/T = 8, the experimental data is corrected for the difference between the origin, O, and the section's vertical center-of-gravity, CG, as outlined by Vugts (1968). In these cases, a note has been included in the plot legend. The computational results were also obtained about the origin, or CG, to maintain consistency with Vugts' conventions. Results about the origin when B/T = 4 and B/T = 8 were obtained by setting the VCG equal to the draft. In all other cases, the VCG was taken at 0.2 m as indicated. In all cases, a wave heading of 90 degrees was used to match the experimental conditions.

Box Section

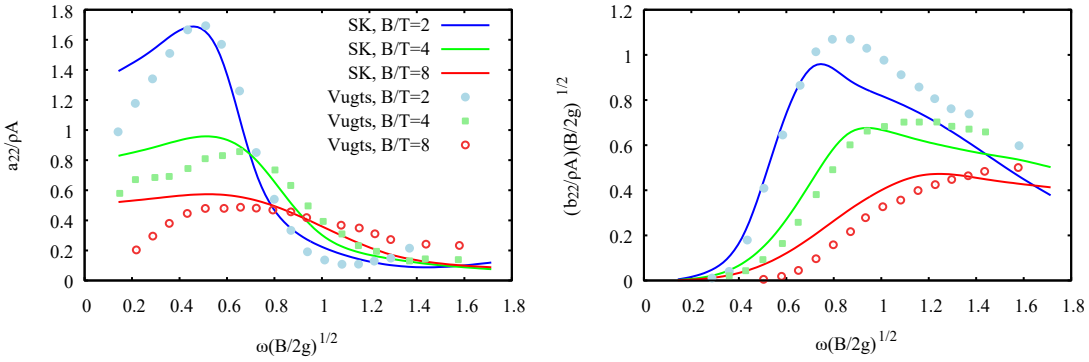

Figure 2. Sway Added Mass and Damping (a_{22}/b_{22}) – Box Section

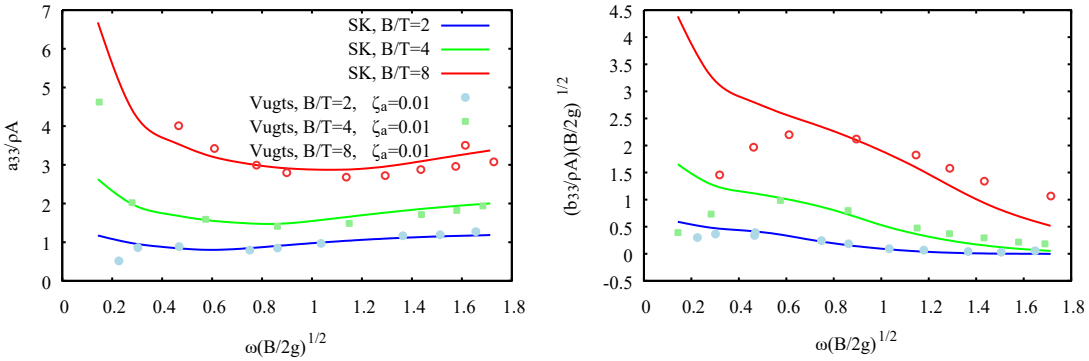

Figure 3. Heave Added Mass and Damping (a_{33}/b_{33}) – Box Section

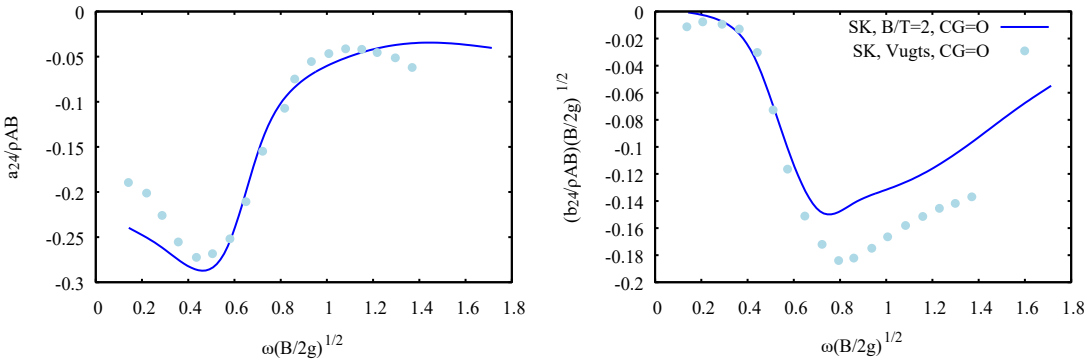

Figure 4. Sway-into-Roll Added Mass and Damping Coefficient (a_{24}/b_{24}) – Box Section, $B/T = 2$

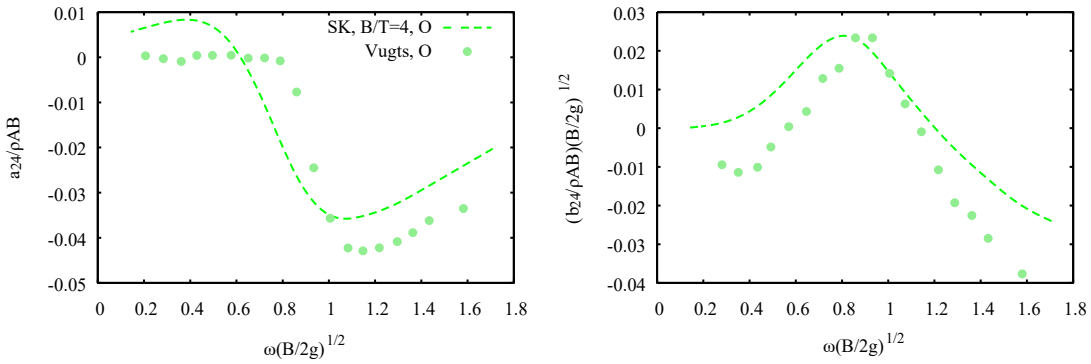

Figure 5. Sway-into-Roll Added Mass and Damping Coefficient (a_{24}/b_{24}) – Box Section, B/T = 4

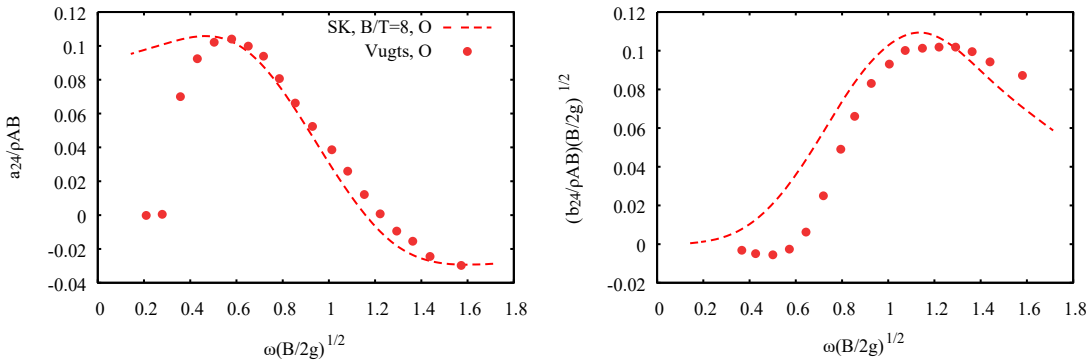

Figure 6. Sway-into-Roll Added Mass and Damping Coefficient (a_{24}/b_{24}) – Box Section, B/T = 8

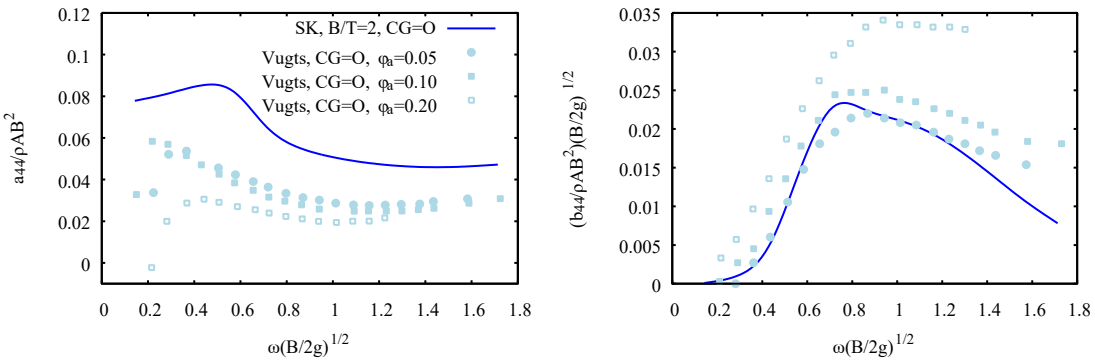

Figure 7. Roll Added Mass Moment of Inertia and Damping Coefficient (a_{44}/b_{44}) – Box Section, B/T = 2

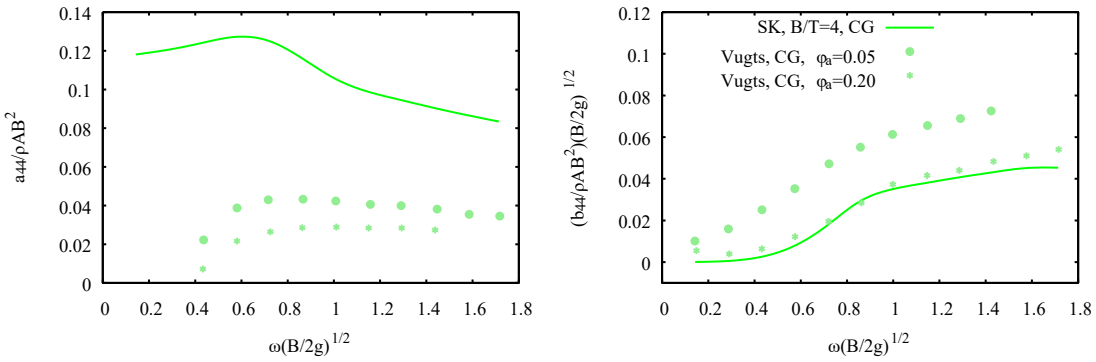

Figure 8. Roll Added Mass Moment of Inertia and Damping Coefficient (a_{44}/b_{44}) – Box Section, B/T = 4

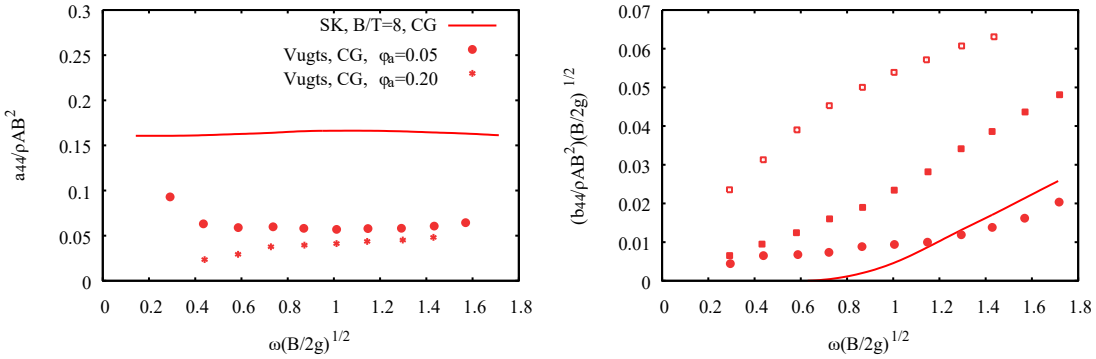

Figure 9. Roll Added Mass Moment of Inertia and Damping Coefficient (a_{44}/b_{44}) – Box Section, B/T = 8

Triangle Section

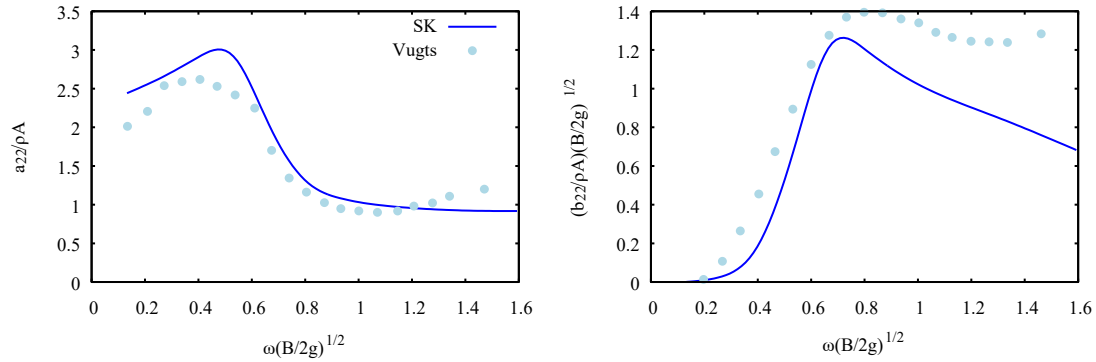

Figure 10. Sway Added Mass and Damping Coefficient (a_{22}/b_{22}) – Triangle Section

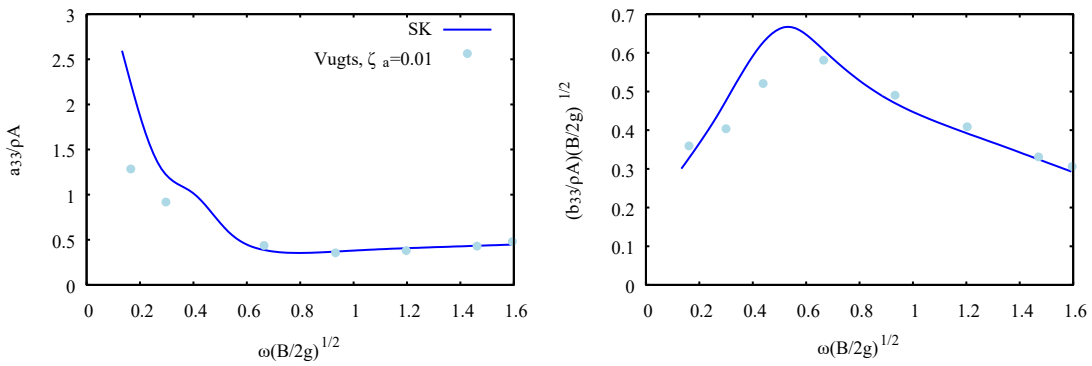

Figure 11. Heave Added Mass and Damping Coefficient (a_{33}/b_{33}) – Triangle Section

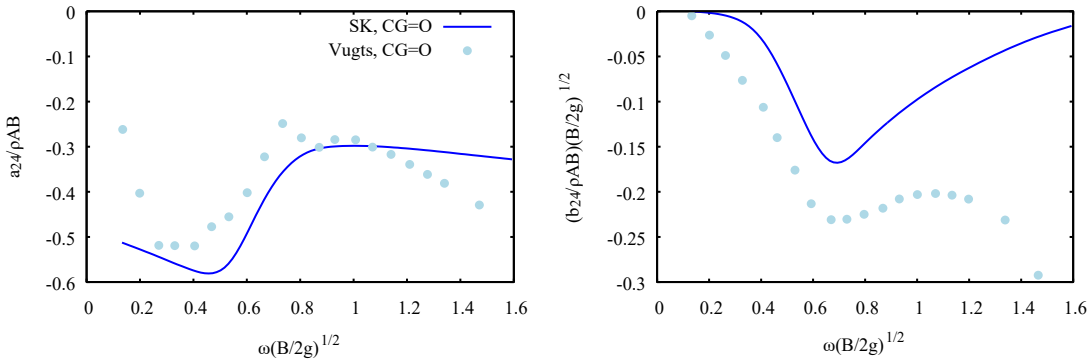

Figure 12. Sway-into-Roll Added Mass and Damping Coefficient (a_{24}/b_{24}) – Triangle Section

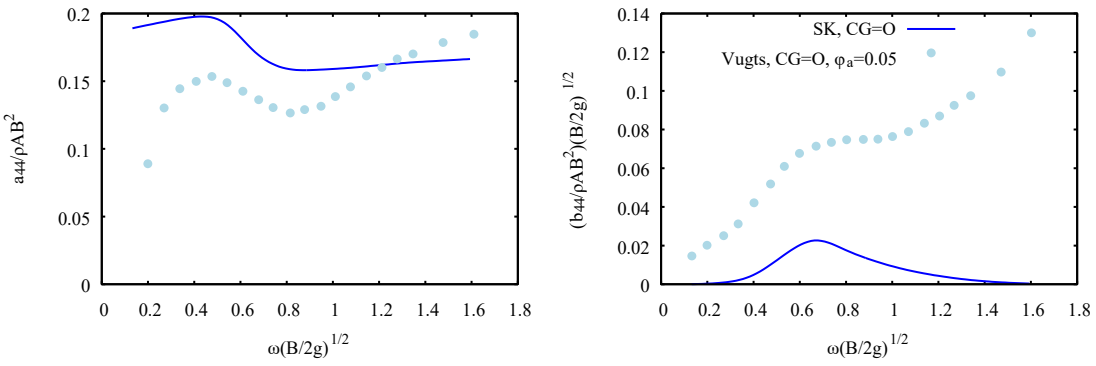

Figure 13. Roll Added Mass Moment of Inertia and Damping Coefficient (a_{44}/b_{44}) – Triangle Section

Cylindrical Section

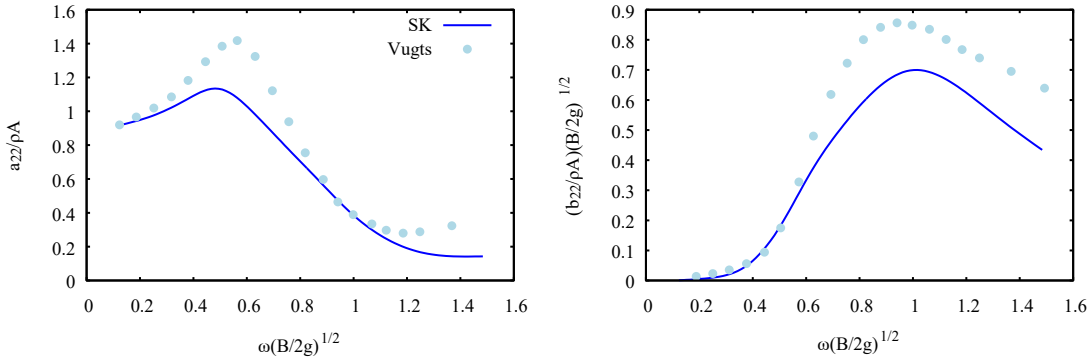

Figure 14. Sway Added Mass and Damping Coefficient (a_{22}/b_{22}) – Cylinder Section

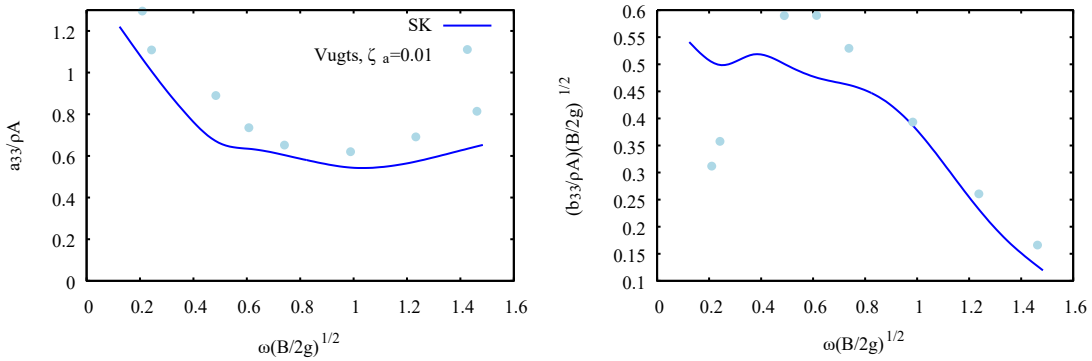

Figure 15. Heave Added Mass and Damping Coefficient (a_{33}/b_{33}) – Cylinder Section

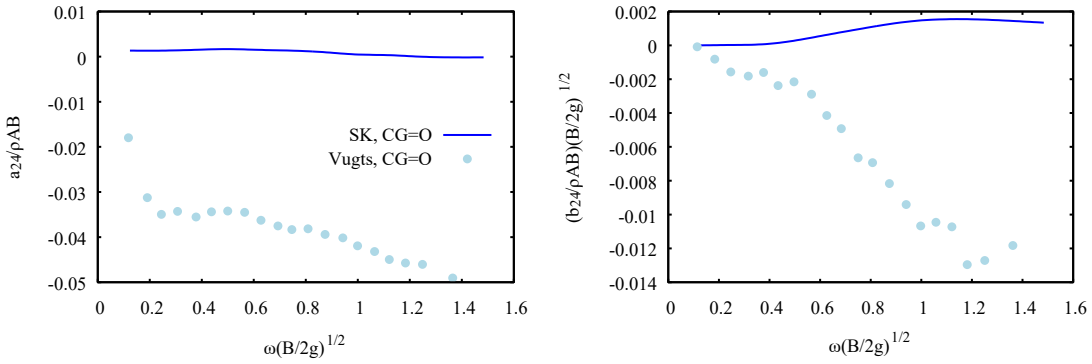

Figure 16. Sway-into-Roll Added Mass and Damping Coefficient (a_{24}/b_{24}) – Cylinder Section

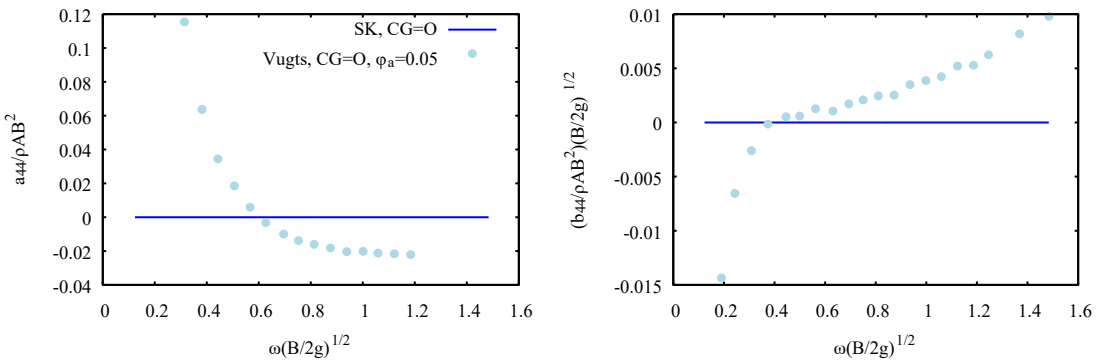

Figure 17. Roll Added Mass Moment of Inertia and Damping Coefficient (a_{44}/b_{44}) – Cylinder Section

3D Forces and Phase Angles at Multiple Headings for Simple Barge Geometries

The three-dimensional wave excitation force and moment amplitudes and phase angles were compared with results from the 3D diffraction panel code DELFRAC. The data used in this study was digitized from plots published by J.M.J. Journée, see "References and Additional Resources". Two different "barge-like" geometries were used: a box-barge and a triangular barge. The box-barge has a beam of 30 m, a length of 300 m, and a draft of 15 m, yielding a beam-to-draft ratio of 2. The VCG was set at the waterline, or 15 m. The triangular barge had beam of 34.64 m, a length of 300 m, and a draft of 30 m. The barges were evaluated at wave headings of 0, 30, 60, and 90 degrees. Forward speed is zero and water depth is infinite. The beam factor and length factor (see the SK User's Manual for details) were left at the default values of 8.0 and 50.0, respectively.

The results are shown by Figure 18 through Figure 41. In all cases, the agreement is quite satisfactory. Because SeaKeeping uses a more robust treatment of the normal vectors than other strip-theory codes, it is able to capture more of the 3D effects. This appears to be most evident at higher frequencies, where diffraction typically plays a greater role in the total forcing.

Due to the symmetry of the barge geometries, the sway and roll forcing are zero at a wave heading of zero degrees, as evidenced by the seemingly blank plot. The phase angles at these headings are meaningless and are therefore omitted.

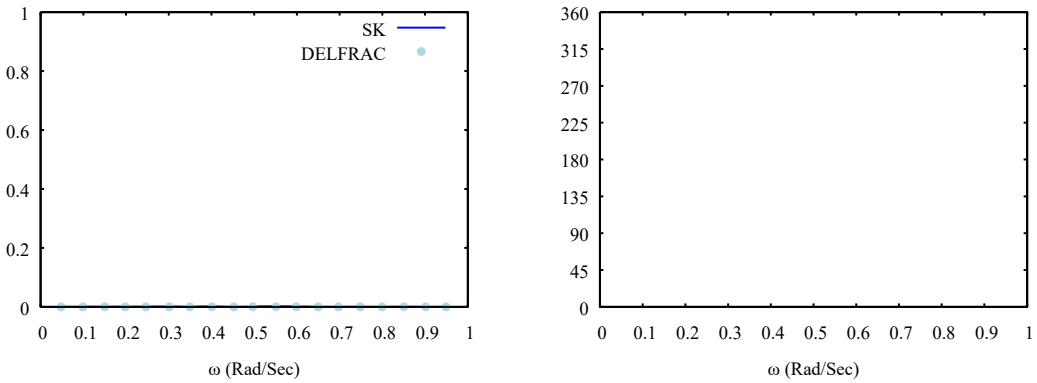

Figure 18. Sway Forcing Amplitude and Phase, Heading: 0° - Box Barge

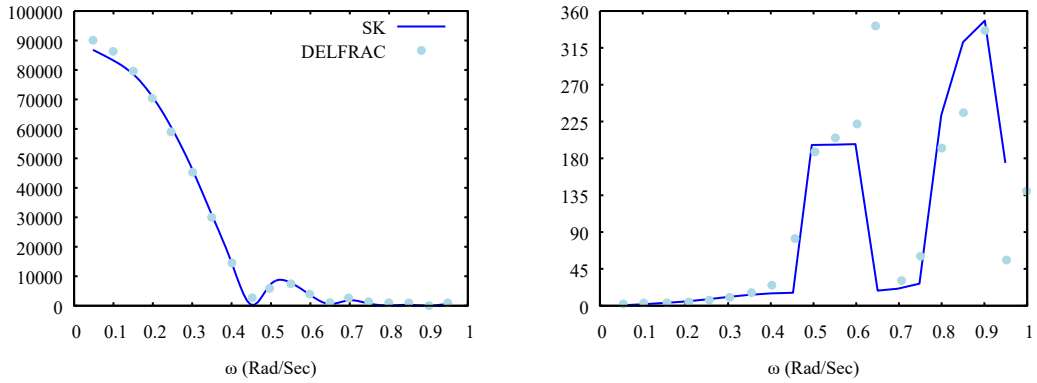

Figure 19. Heave Forcing Amplitude and Phase, Heading: 0° - Box Barge

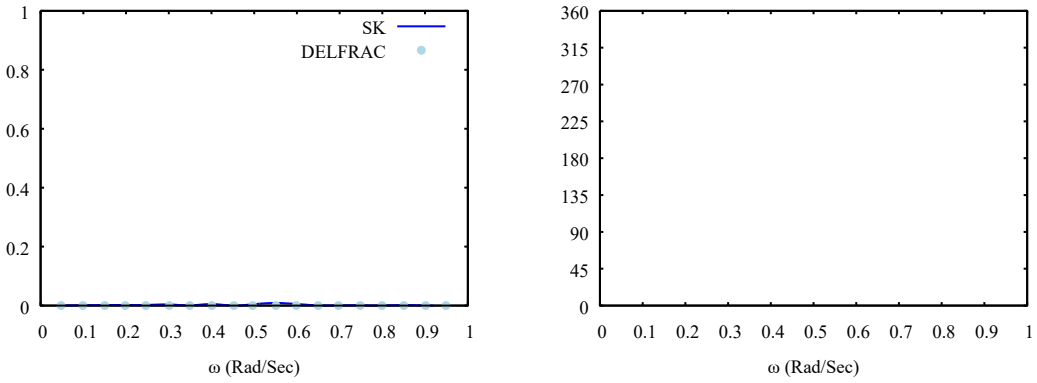

Figure 20. Roll Moment Amplitude and Phase, Heading: 0° - Box Barge

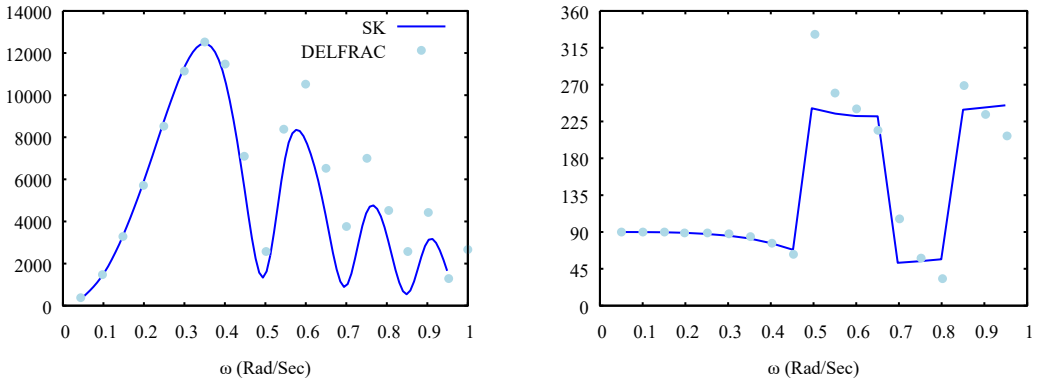

Figure 21. Sway Forcing Amplitude and Phase, Heading: 30° - Box Barge

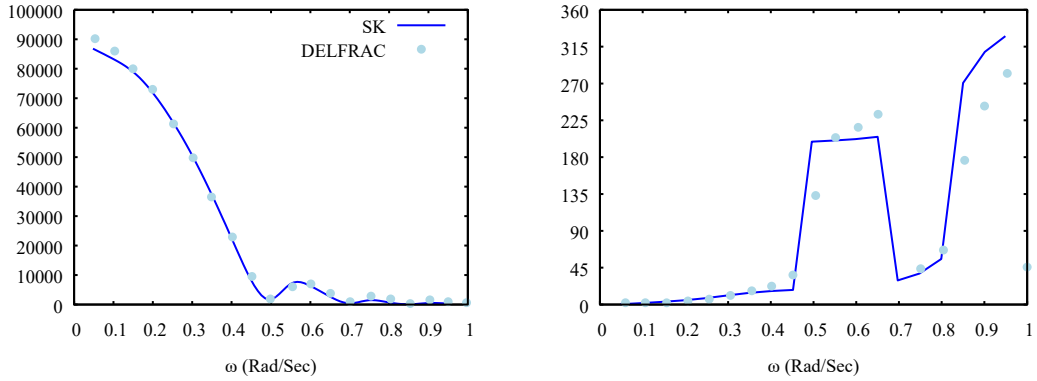

Figure 22. Heave Forcing Amplitude and Phase, Heading: 30° - Box Barge

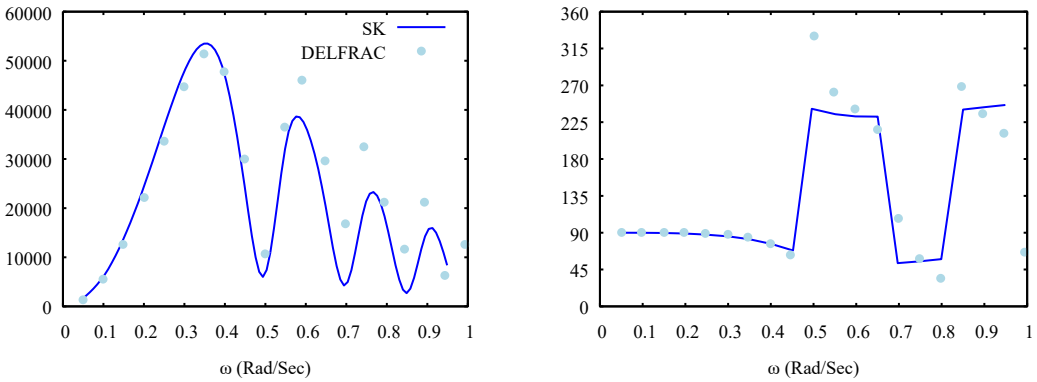

Figure 23. Roll Moment Amplitude and Phase, Heading: 30° - Box Barge

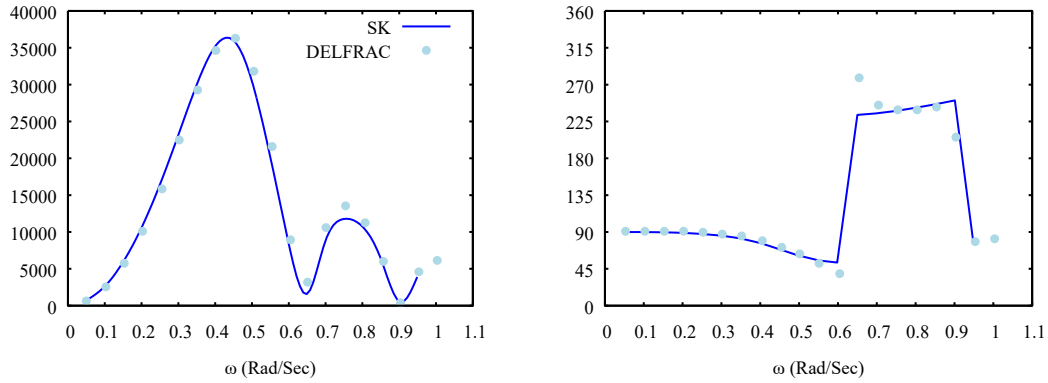

Figure 24. Sway Forcing Amplitude and Phase, Heading: 60° - Box Barge

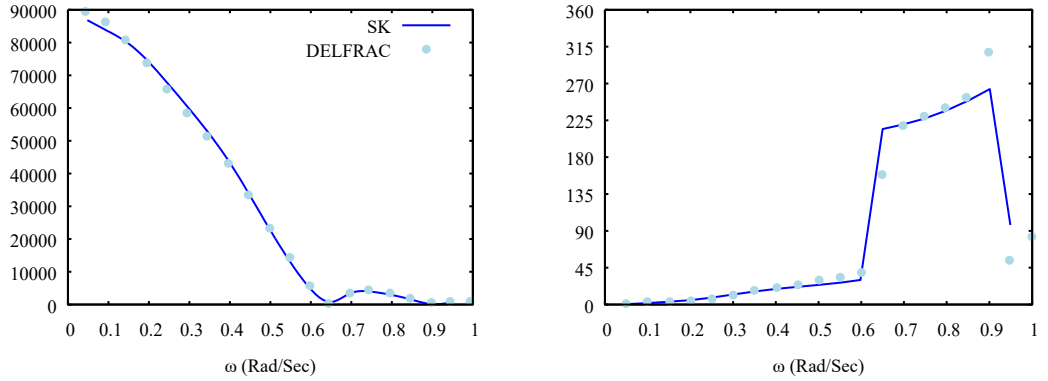

Figure 25. Heave Forcing Amplitude and Phase, Heading: 60° - Box Barge

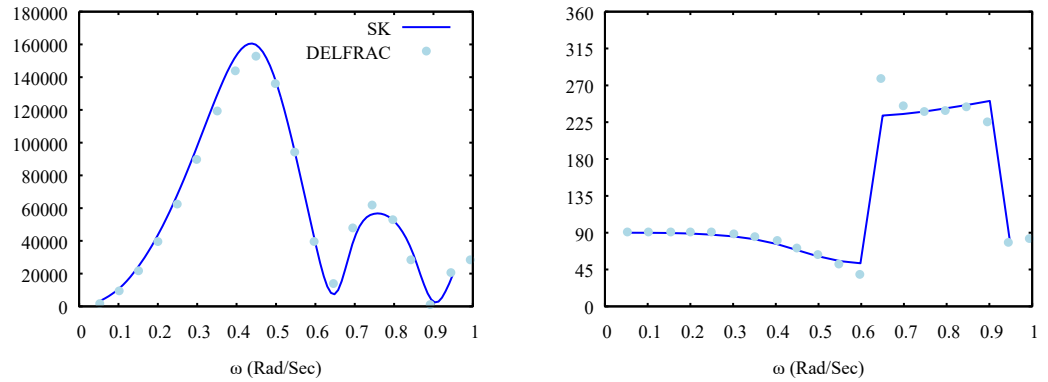

Figure 26. Roll Moment Amplitude and Phase, Heading: 60° - Box Barge

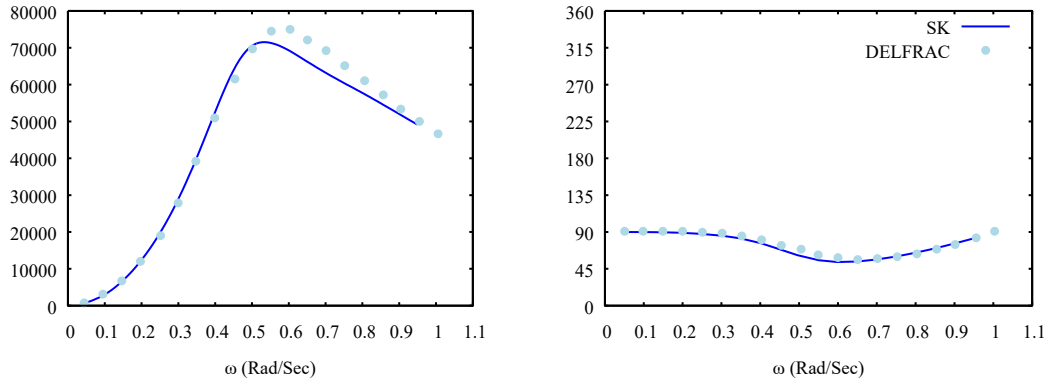

Figure 27. Sway Forcing Amplitude and Phase, Heading: 90° - Box Barge

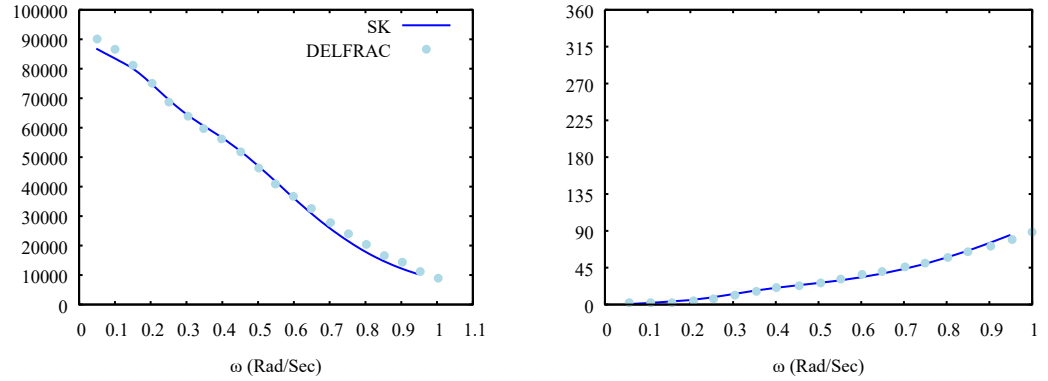

Figure 28. Heave Forcing Amplitude and Phase, Heading: 90° - Box Barge

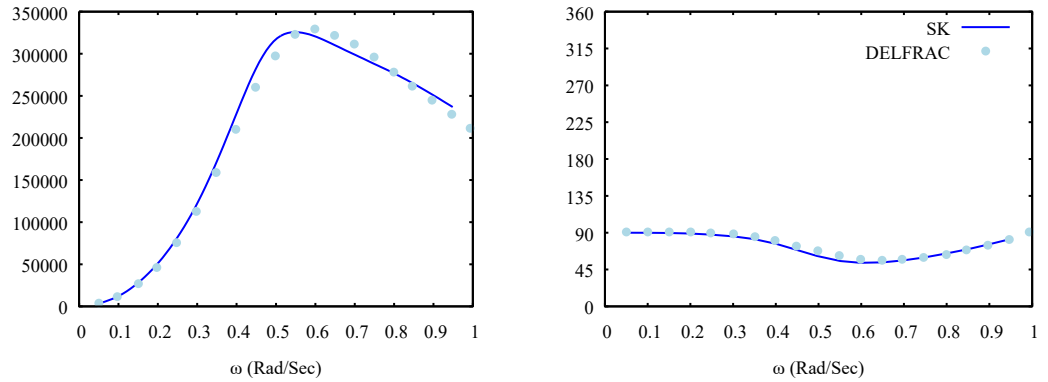

Figure 29. Roll Moment Amplitude and Phase, Heading: 90° - Box Barge

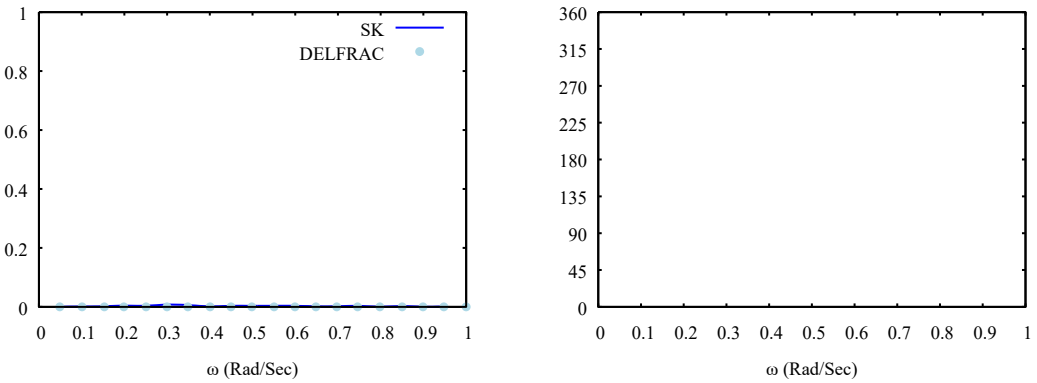

Figure 30. Sway Forcing Amplitude and Phase, Heading: 0° - Triangle Barge

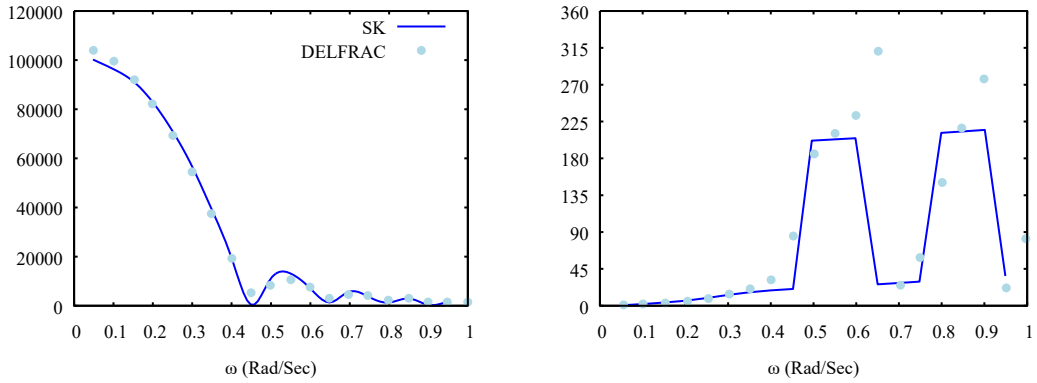

Figure 31. Heave Forcing Amplitude and Phase, Heading: 0° – Triangle Barge

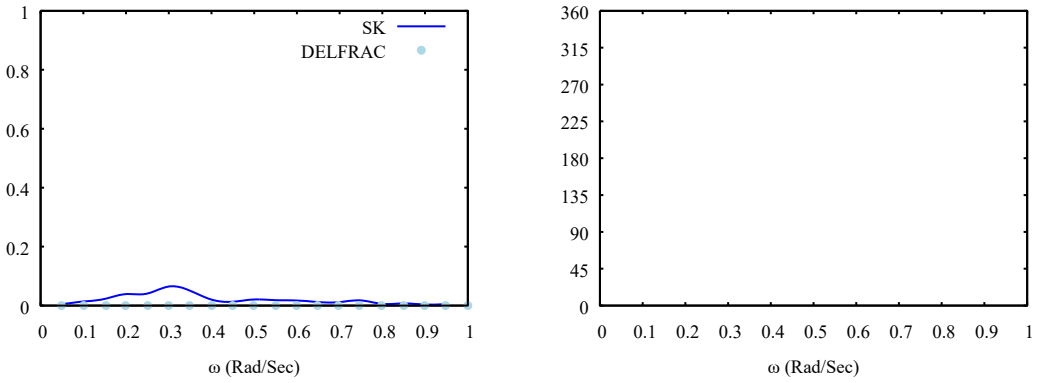

Figure 32. Roll Moment Amplitude and Phase, Heading: 0° - Triangle Barge

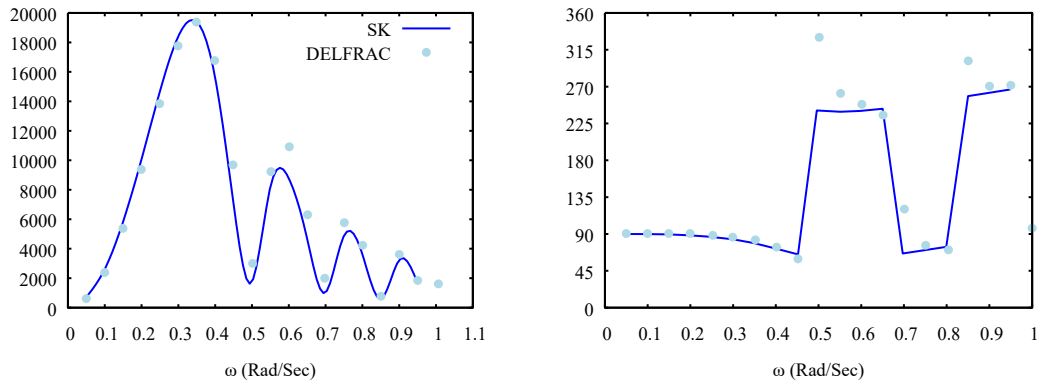

Figure 33. Sway Forcing Amplitude and Phase, Heading: 30° - Triangle Barge

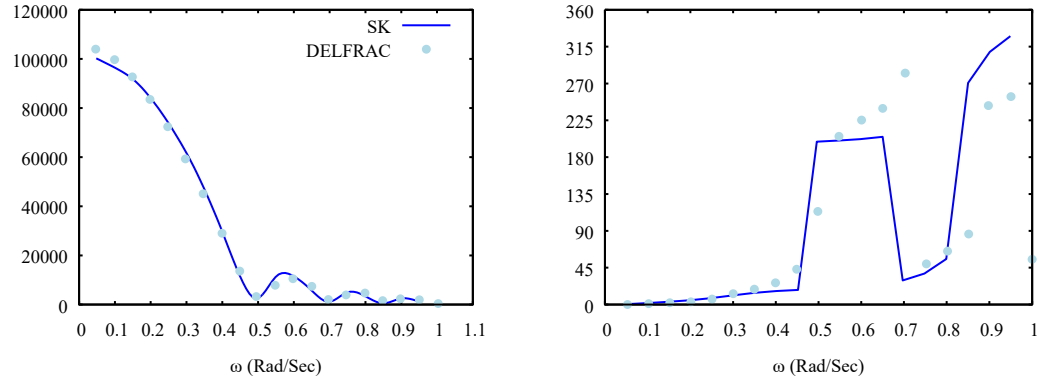

Figure 34. Heave Forcing Amplitude and Phase, Heading: 30° - Triangle Barge

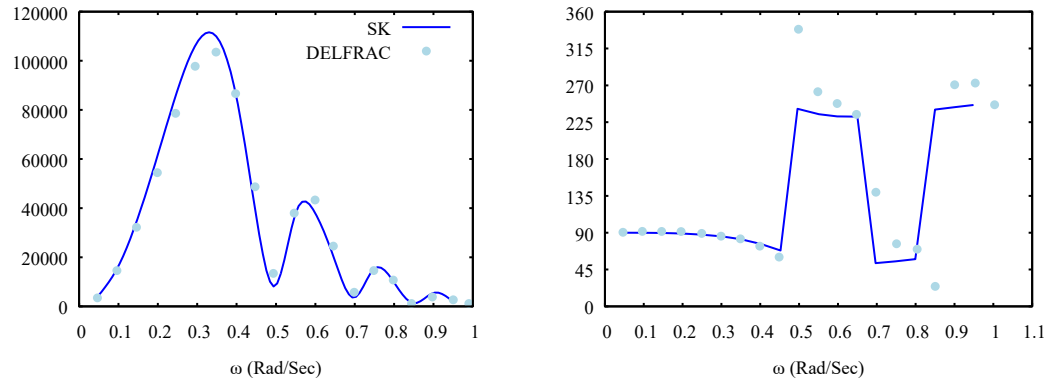

Figure 35. Roll Moment Amplitude and Phase, Heading: 30° - Triangle Barge

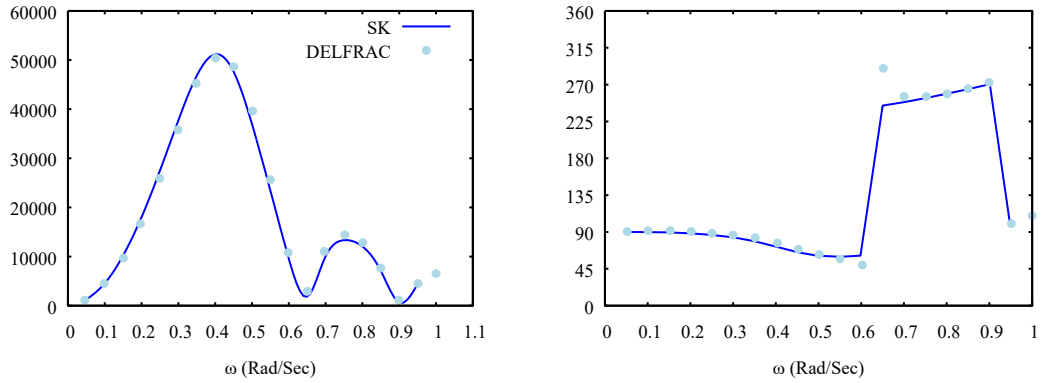

Figure 36. Sway Forcing Amplitude and Phase, Heading: 60° - Triangle Barge

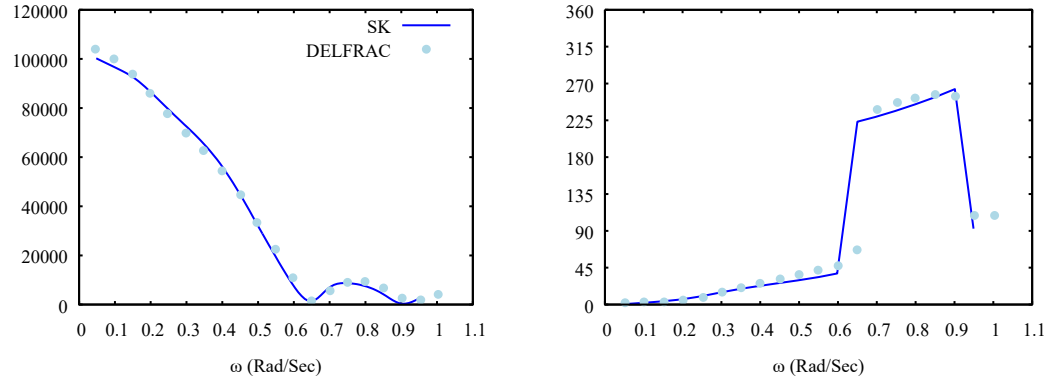

Figure 37. Heave Forcing Amplitude and Phase, Heading: 60° - Triangle Barge

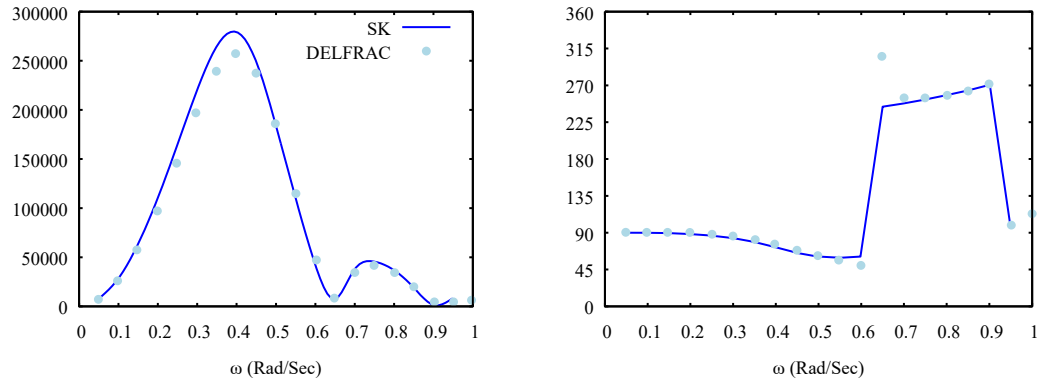

Figure 38. Roll Moment Amplitude and Phase, Heading: 60° - Triangle Barge

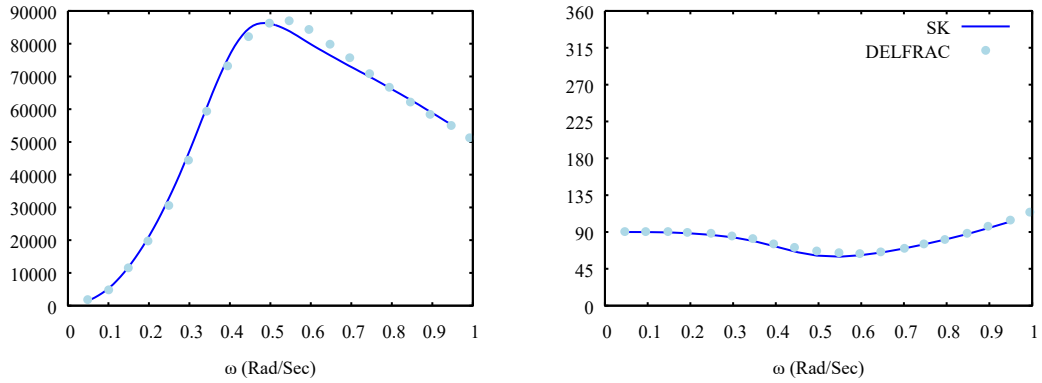

Figure 39. Sway Forcing Amplitude and Phase, Heading: 90° - Triangle Barge

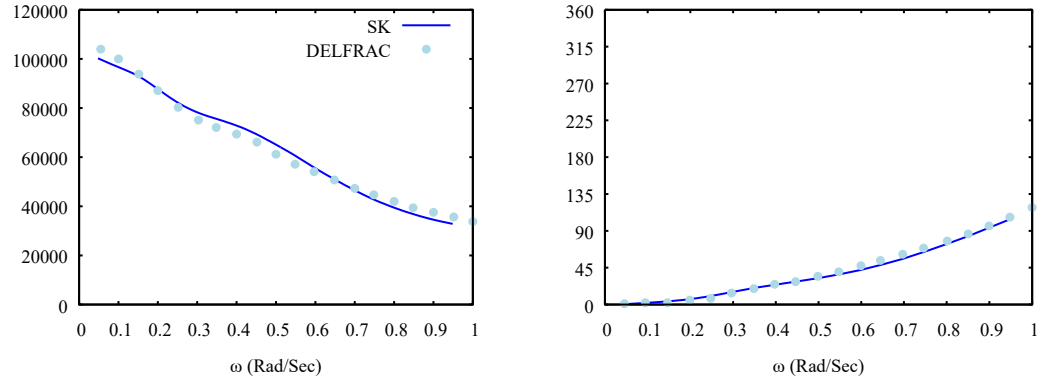

Figure 40. Heave Forcing Amplitude and Phase, Heading: 90° - Triangle Barge

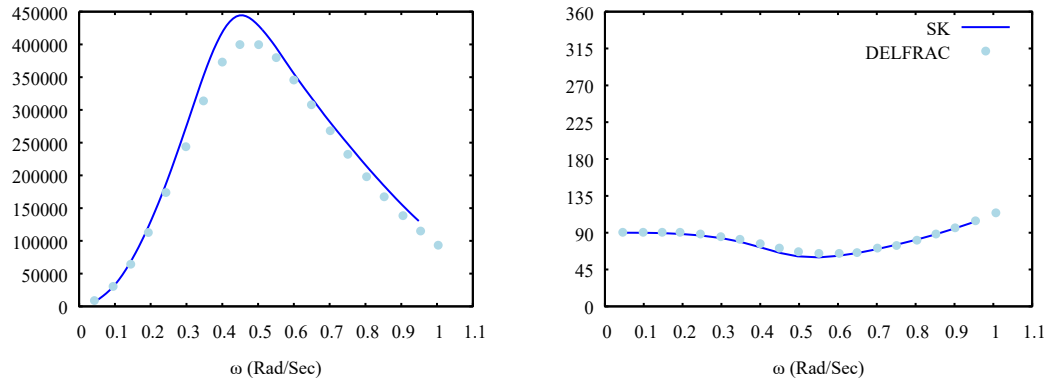

Figure 41. Roll Moment Amplitude and Phase, Heading: 90° - Triangle Barge

3D Forces and Phase Angles at Multiple Headings for a Tanker Hull

The three-dimensional total forcing amplitudes and phase angles for the full-scale crude oil tanker hull “Macoma” were computed and compared to data from the 3D panel method code DELFRAC. The data used in this study was digitized from plots published by J.M.J. Journée (2001). An isometric view and body plan of the submerged hull geometry are given by Figure 42. The geometry file was developed from poor quality digitized lines drawings, so some error is expected in the conversion of the lines to the geometry file. Section Editor was utilized to develop and edit the model, and additional stations were added using the built-in interpolation feature. The origin was placed at the aft-most station shown in the isometric and body view.

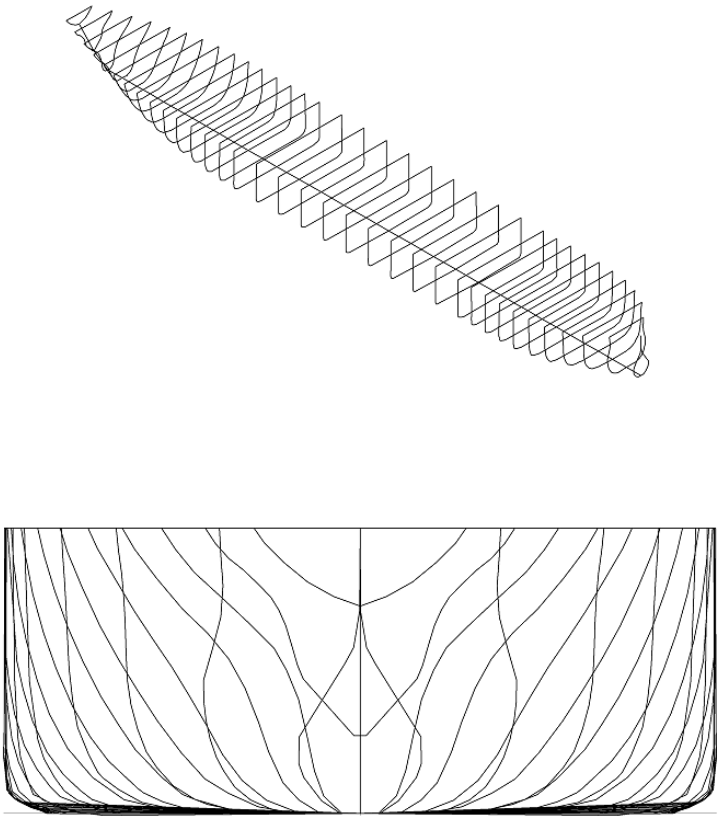

Figure 42. Crude Oil Tanker "Macoma" Submerged Hull Geometry

The hull dimensions and loading condition are given in Table 1. The hull is assumed to be in deep water.

L_{OA}	310.0	m	LCG	163.648	m, fwd *0*
L_{WL}	310.0	m	TCG	0.0	m, *0*
B_{WL}	47.384	m	VCG	18.900	m, *0*
Δ	239,034.88	MT	LCF	156.899	m, fwd *0*
C_B	0.832	-	GM_T	0.392	m
Draft	18.90	m	k_4	18.998	m
Trim	0.0	Deg, aft	k_5	77.500	m
Heel	0.0	Deg	k_6	77.500	m

Table 1. Crude Oil Tanker "Macoma" Details

The hull was subjected to a range of wave frequencies ranging in period from 139.801 sec (0.045 rad/s) to 6.301 sec (1.0 rad/s) with a constant amplitude of 1 meter at wave headings of 0, 30, 60, 90, 120, 150, and 180 degrees. The hull was also held at zero forward speed. The Beam Factor and Length Factor were taken at their default values of 8 and 50, respectively.

The results are plotted against the DELFRAC data in Figure 43 through Figure 63. In most cases, very good agreement is observed. At wave headings of 0° and 180°, the forcing amplitudes in sway are effectively zero, therefore the phase angles are omitted.

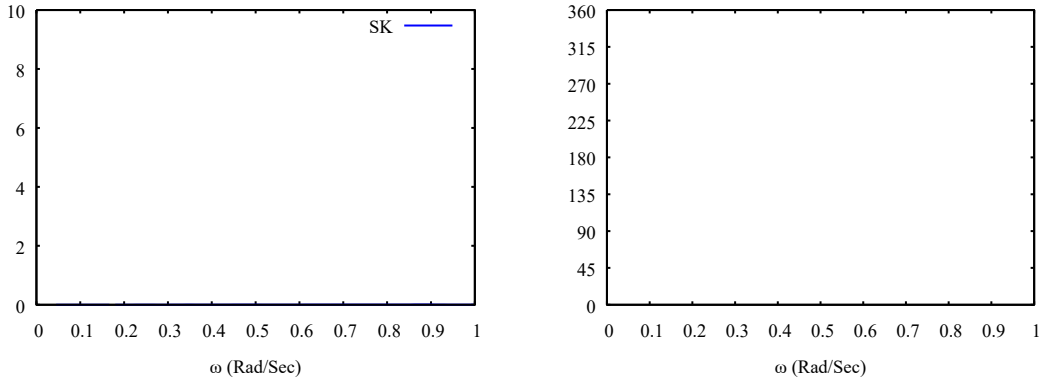

Figure 43. Sway Forcing Amplitude and Phase, Heading: 0°

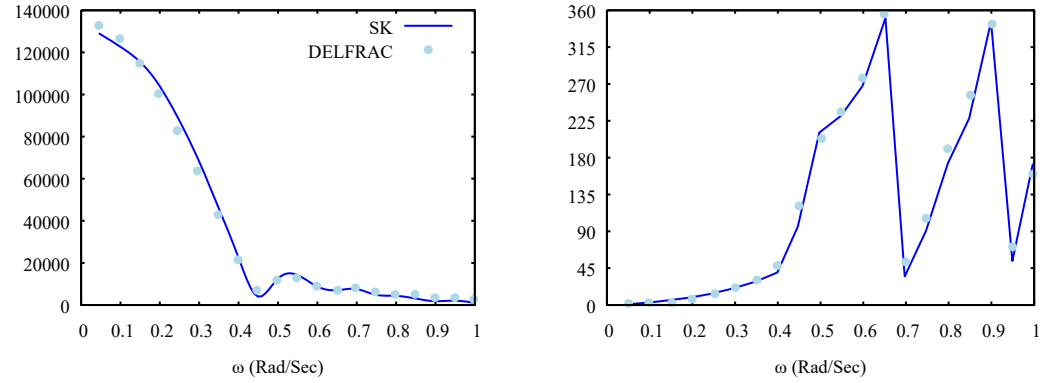

Figure 44. Heave Forcing Amplitude and Phase, Heading: 0°

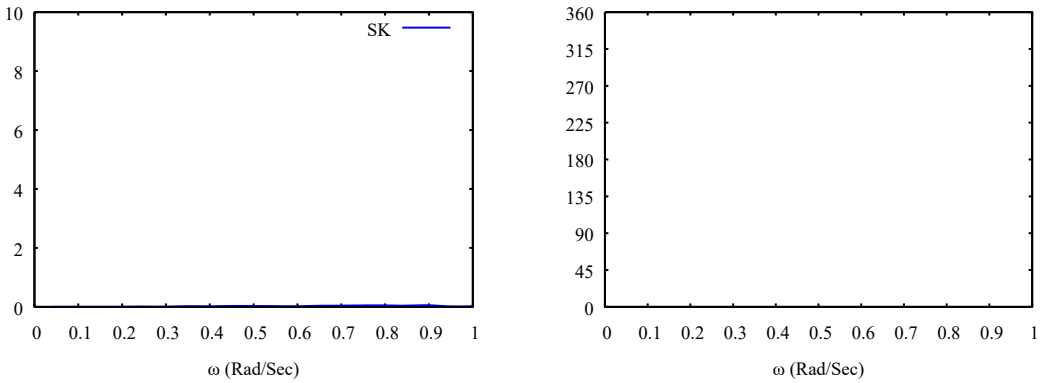

Figure 45. Roll Forcing Amplitude and Phase, Heading: 0°

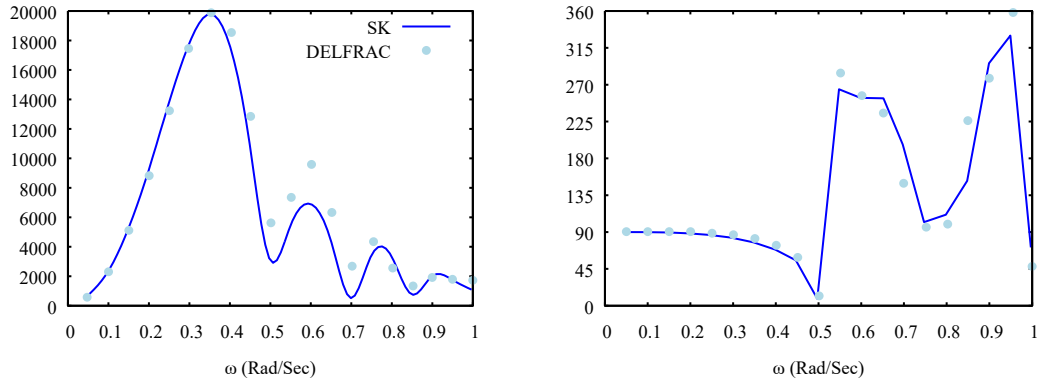

Figure 46. Sway Forcing Amplitude and Phase, Heading: 30°

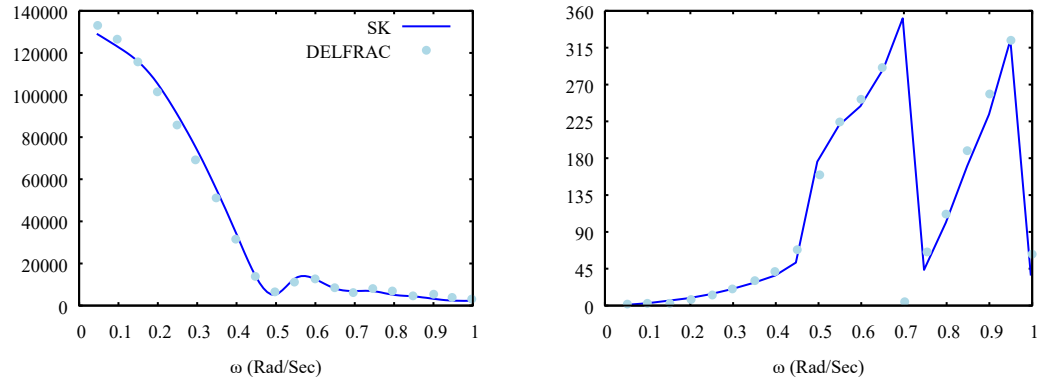

Figure 47. Heave Forcing Amplitude and Phase, Heading: 30°

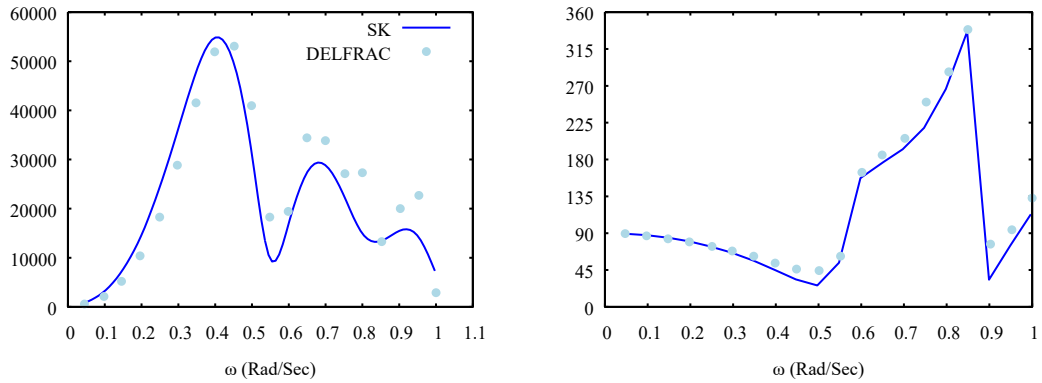

Figure 48. Roll Forcing Amplitude and Phase, Heading: 30°

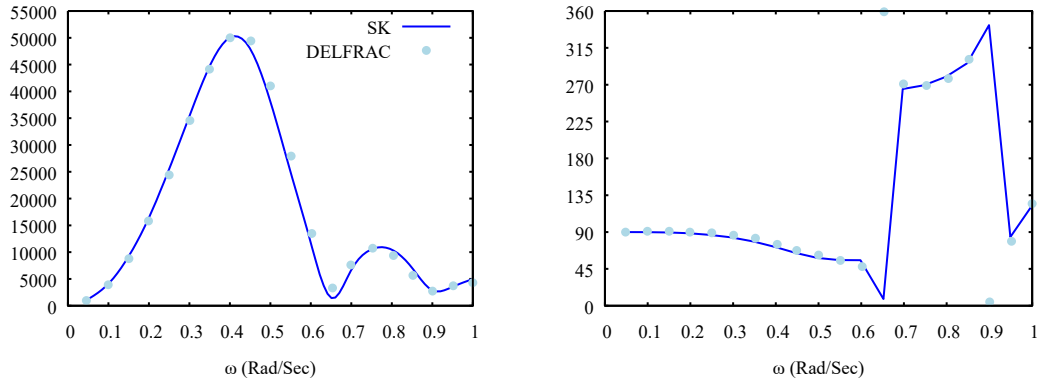

Figure 49. Sway Forcing Amplitude and Phase, Heading: 60°

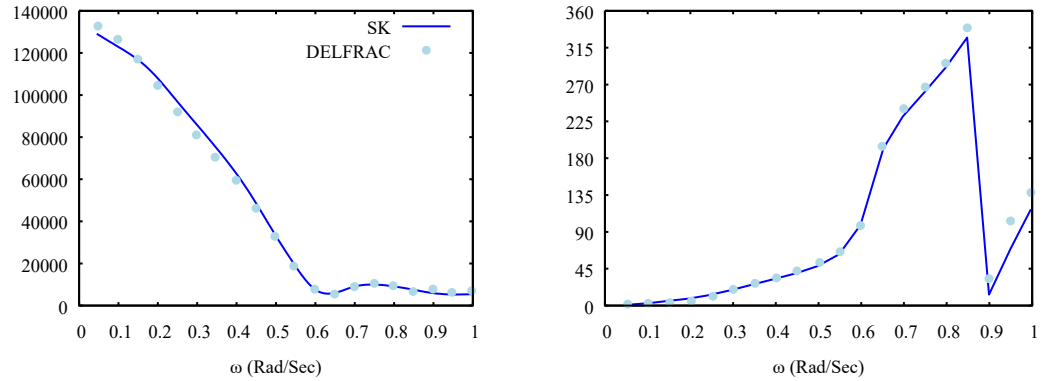

Figure 50. Heave Forcing Amplitude and Phase, Heading: 60°

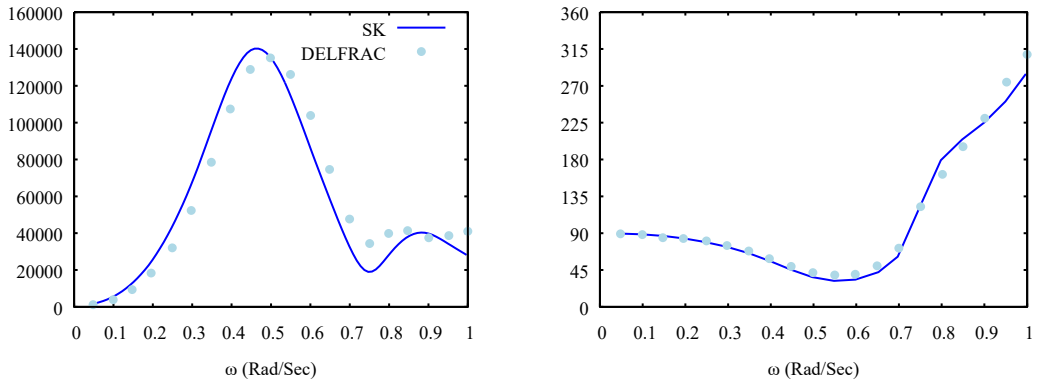

Figure 51. Roll Forcing Amplitude and Phase, Heading: 60°

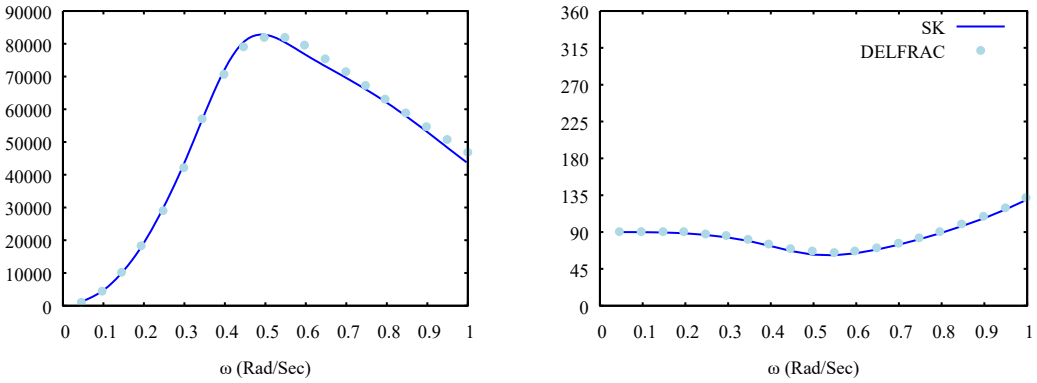

Figure 52. Sway Forcing Amplitude and Phase, Heading: 90°

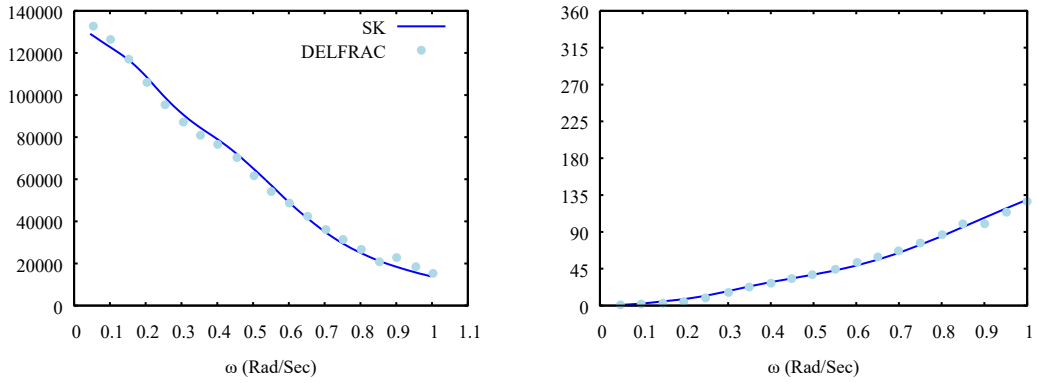

Figure 53. Heave Forcing Amplitude and Phase, Heading: 90°

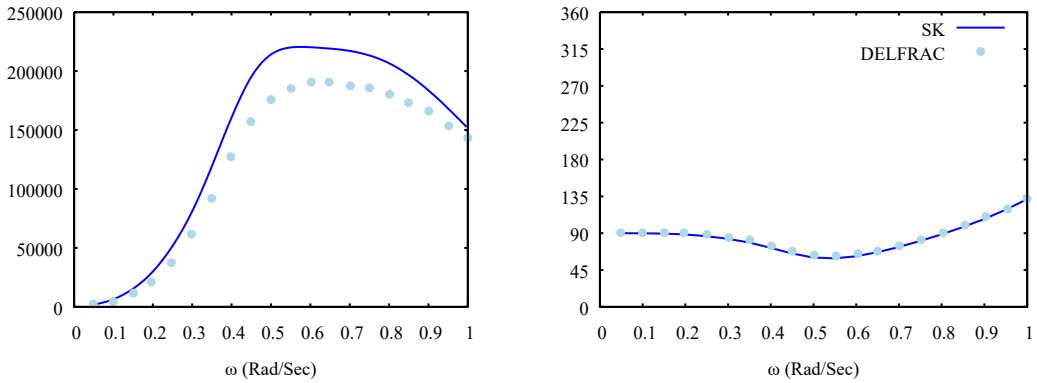

Figure 54. Roll Forcing Amplitude and Phase, Heading: 90°

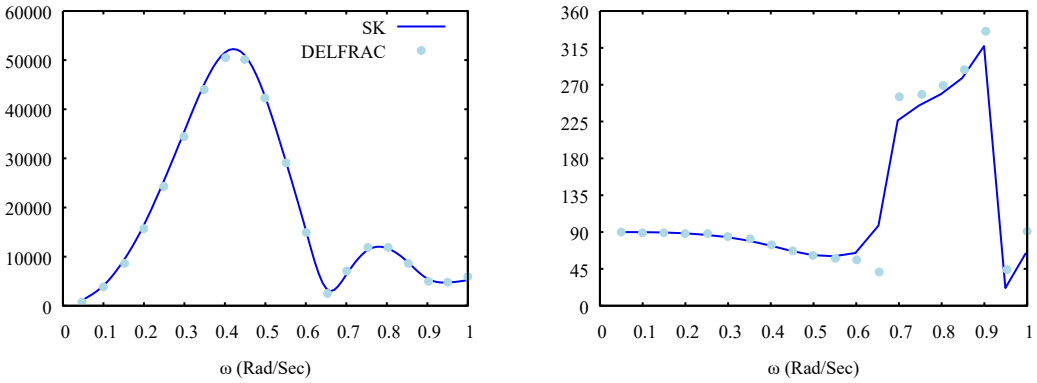

Figure 55. Sway Forcing Amplitude and Phase, Heading: 120°

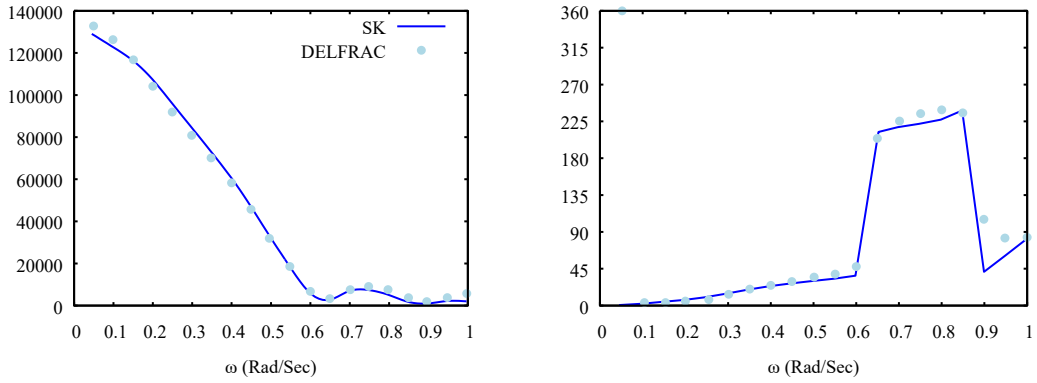

Figure 56. Heave Forcing Amplitude and Phase, Heading: 120°

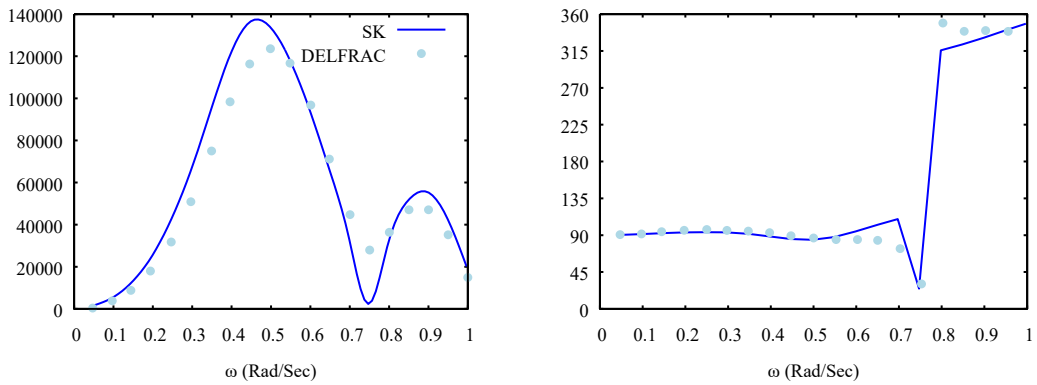

Figure 57. Roll Forcing Amplitude and Phase, Heading: 120°

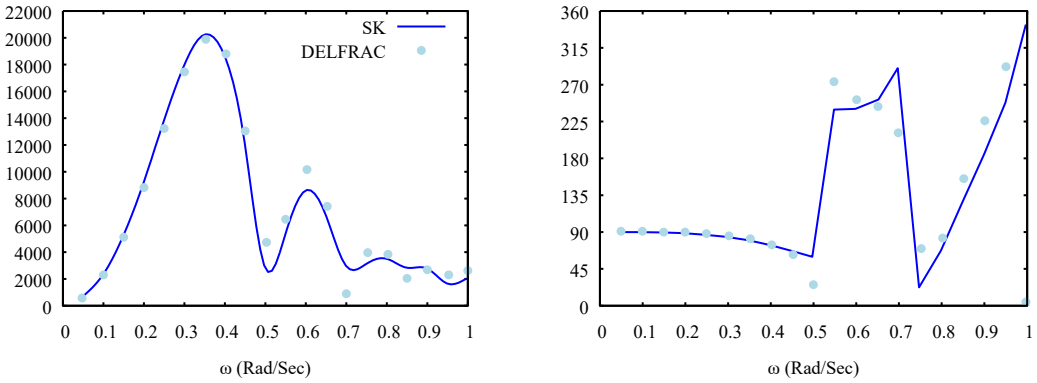

Figure 58. Sway Forcing Amplitude and Phase, Heading: 150°

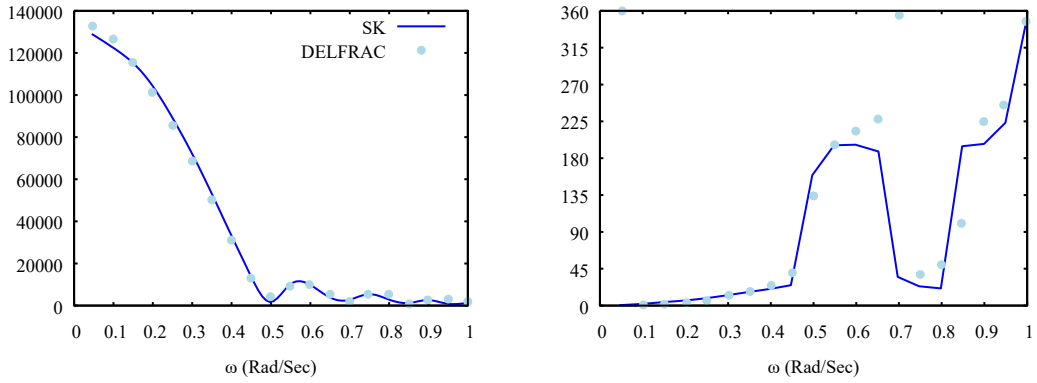

Figure 59. Heave Forcing Amplitude and Phase, Heading: 150°

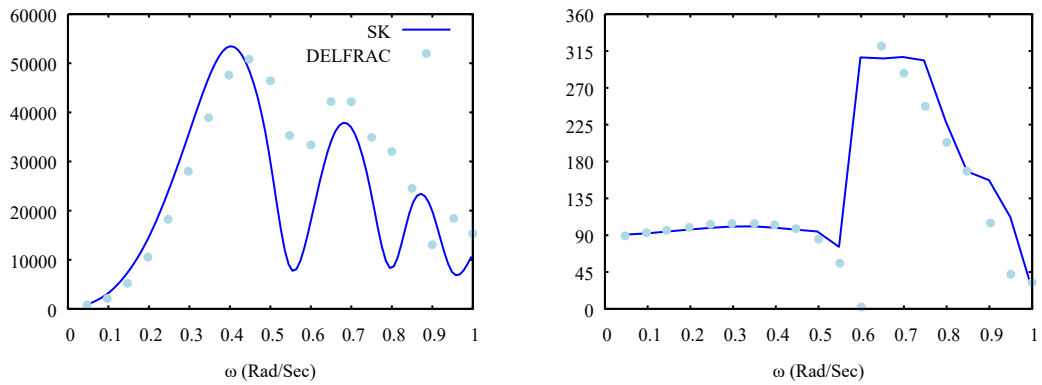

Figure 60. Roll Forcing Amplitude and Phase, Heading: 150°

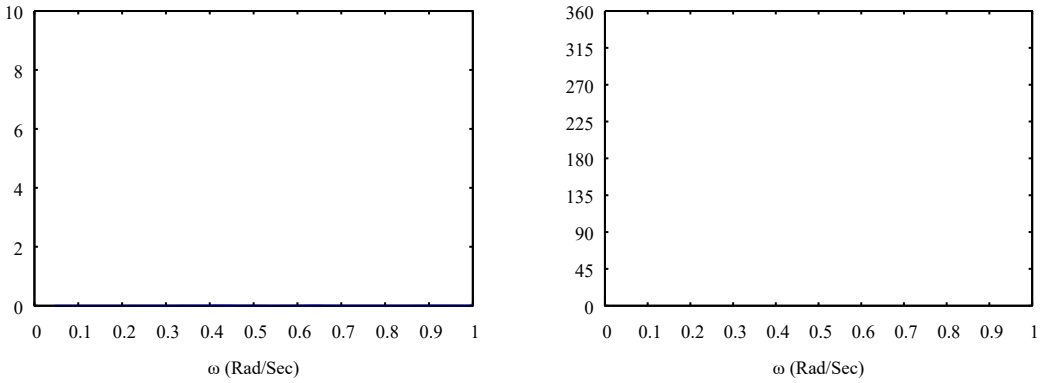

Figure 61. Sway Forcing Amplitude and Phase, Heading: 180°

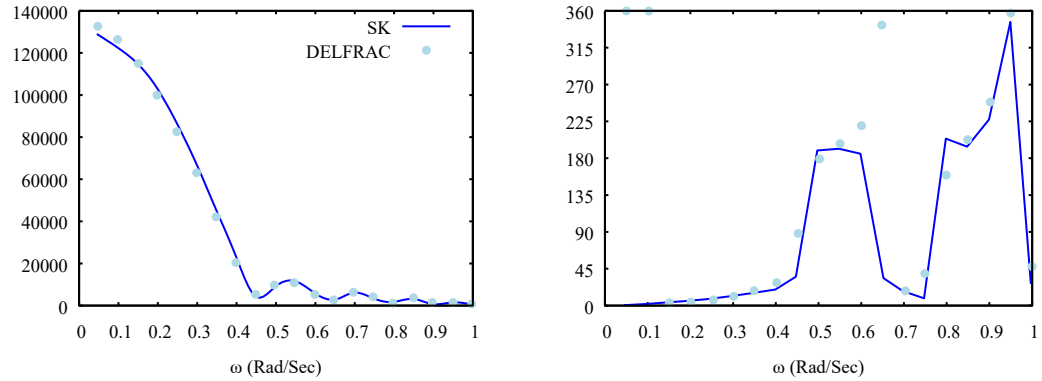

Figure 62. Heave Forcing Amplitude and Phase, Heading: 180°

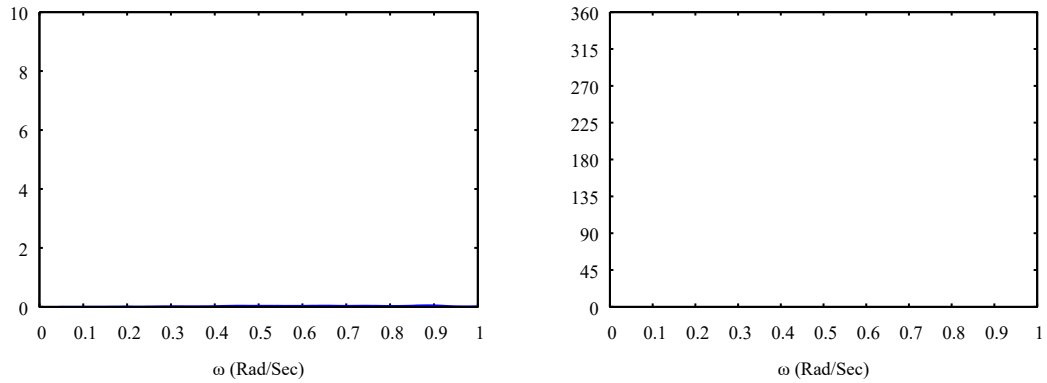

Figure 63. Roll Forcing Amplitude and Phase, Heading: 180°

Absolute and Relative RAOs and Accelerations for the Flokstra Containership

The heave, pitch, and roll absolute RAOs, relative heave RAOs, and vertical accelerations were computed for several Critical Points on the full-scale Flokstra containership hull. The responses computed by SeaKeeping were then compared to model test data obtained by (Zhou, Zhou, & Xie, 1996) at the seakeeping basin at the China Ship Scientific Research Center (CSSRC).

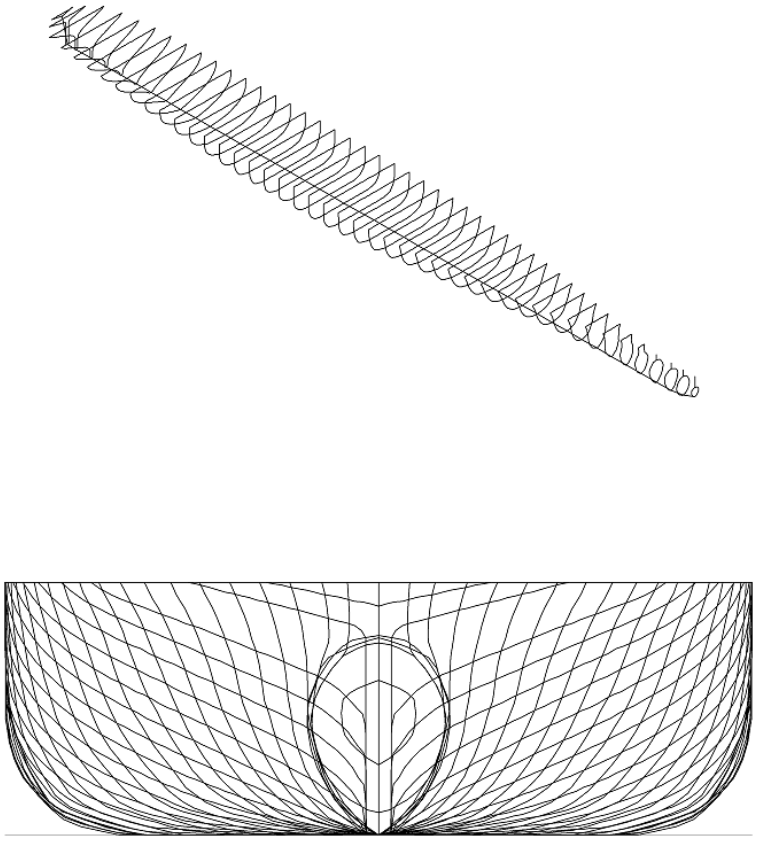

Figure 64. Flokstra Containership Submerged Hull Geometry

The responses were computed for two different forward speeds: 10 knots (Fr=0.10) and 22 knots (Fr=0.22). In addition, wave headings of 180, 135, and 90 degrees in deep water were analyzed. An isometric view and body plan of the hull are given by Figure 64. The hull offsets were digitized from scanned and printed lines, so there are some imperfections in the model. Additional stations were added using the interpolation features in Section Editor. The origin was placed 10.838 m aft of the forward-most station shown.

The dimensions and loading condition used for the computational results are given by Table 2.

L_{OA}	287.435	m	LCG	150.530	m, aft O
L_{WL}	287.435	m	TCG	0.0	m, O
B_{WL}	32.204	m	VCG	13.490	m, O
Δ	61,911.32	MT	LCF	159.937	m, aft O
C_B	0.60	-	GM_T	1.005	m
Draft	10.85	m	k_4	12.075	m
Trim	0.0	Deg, aft	k_5	66.960	m
Heel	0.0	Deg	k_6	66.960	m

Table 2. Flokstra Containership Details

Table 3 gives the locations of each Critical Point as well as the overall center of gravity (CG). The locations of the points were selected to match, as best as possible, the probe locations on the model during testing.

#	Description	L	T	V
4	Orig. Sta17 CL DK	40.5a	0	18.662
6	Orig. Sta5 Stbd DK	202.5a	16.336s	18.662
8	Orig. Sta10 Stbd DK	135.0a	15.970s	18.662
10	Orig. Sta14 Stbd DK	81.0a	15.510s	18.662
12	Orig. Sta17 Stbd DK	40.4a	14.634s	18.662

Table 3. Flokstra Critical Points

In general, the results show fair to good agreement with the experimental data. Of note is the influence of non-wave potential damping in roll. The experimental work noted a significant increase in roll damping at higher speeds and at 90° wave headings. The computational results do not include any additional roll damping other than wave potential damping. The computational results therefore over-predict the roll response in beam seas, especially at the higher speed, near roll resonance, as evidenced in the roll RAO and relative motion RAOs. In addition, dynamic swell up affects are not included in the computational results, and while the influence of the dynamic waterline was not discussed in the experimental work, it is expected that this accounts for some additional deviation from the computational results. Moreover, there is some ambiguity as to the exact measurement locations of the probes, and noted possibilities for experimental error in the experimental relative responses.

Despite these deviations, the computational results are consistent with expectations, and exhibit useful predictions of the experimental observations.

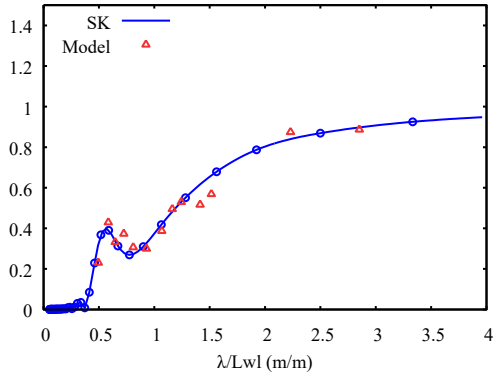

Figure 65. CG – Heave RAO, Speed: 10 kn (Fr=0.1), Heading: 180°

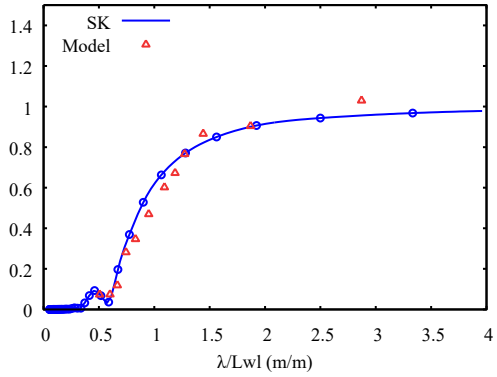

Figure 66. CG – Pitch RAO, Speed: 10 kn (Fr=0.1), Heading: 180°

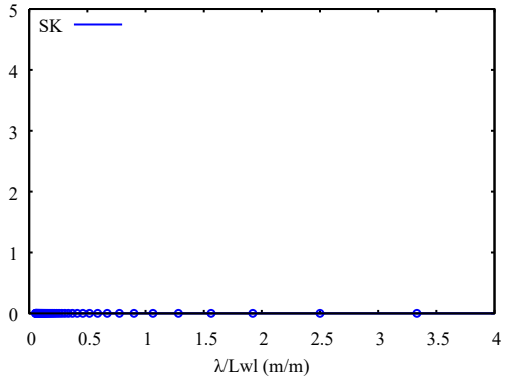

Figure 67. CG – Roll RAO, Speed: 10 kn (Fr=0.1), Heading: 180°

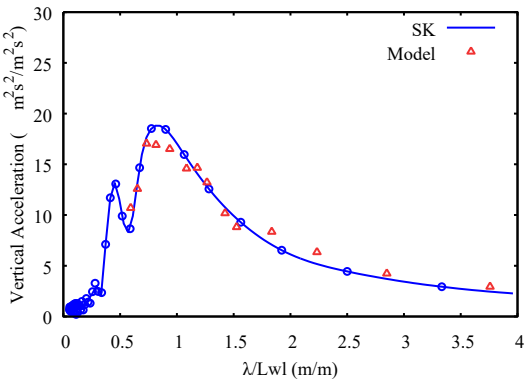

Figure 68. Point 4 – Vertical Acceleration, Speed: 10 kn (Fr=0.1), Heading: 180°

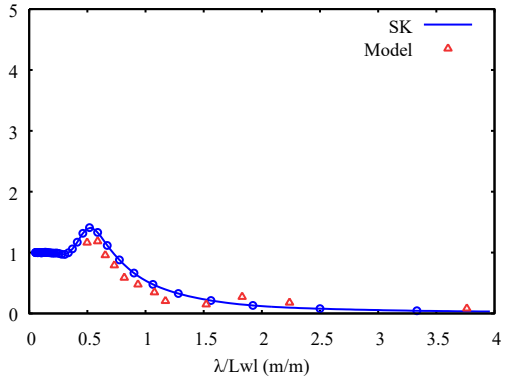

Figure 69. Point 6 – Relative Heave RAO, Speed: 10 kn (Fr=0.1), Heading: 180°

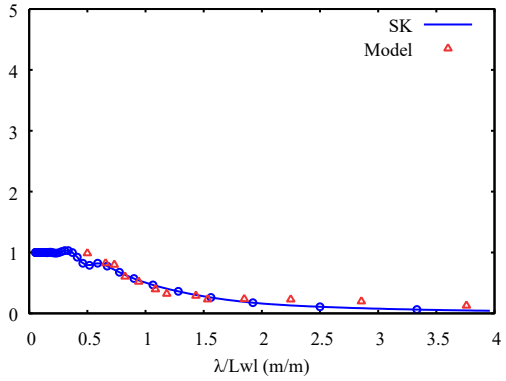

Figure 70. Point 8 – Relative Heave RAO, Speed: 10 kn (Fr=0.1), Heading: 180°

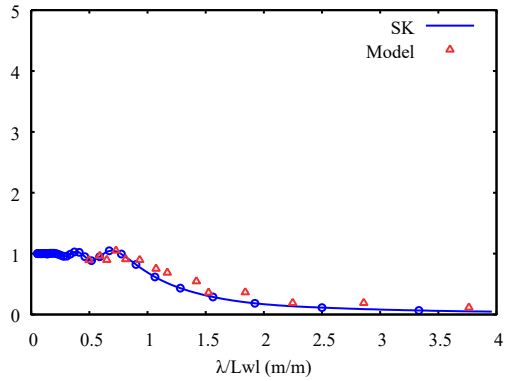

Figure 71. Point 10 – Relative Heave RAO, Speed: 10 kn (Fr=0.1), Heading: 180°

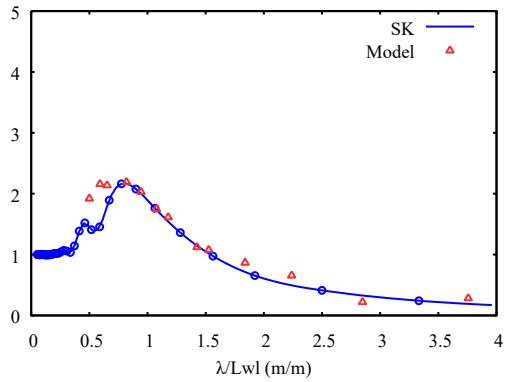

Figure 72. Point 12 – Relative Heave RAO, Speed: 10 kn (Fr=0.1), Heading: 180°

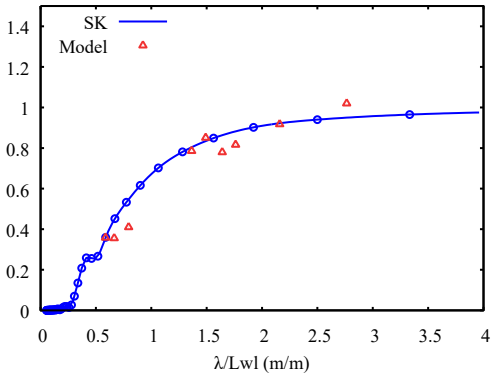

Figure 73. CG – Heave RAO, Speed: 10 kn (Fr=0.1), Heading: 135°

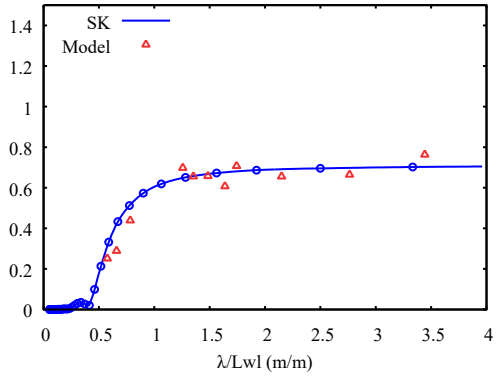

Figure 74. CG – Pitch RAO, Speed: 10 kn (Fr=0.1), Heading: 135°

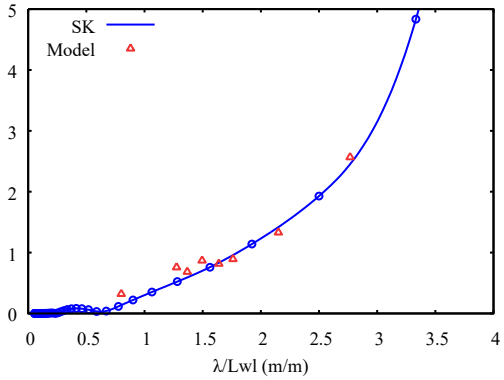

Figure 75. CG – Roll RAO, Speed: 10 kn (Fr=0.1), Heading: 135°

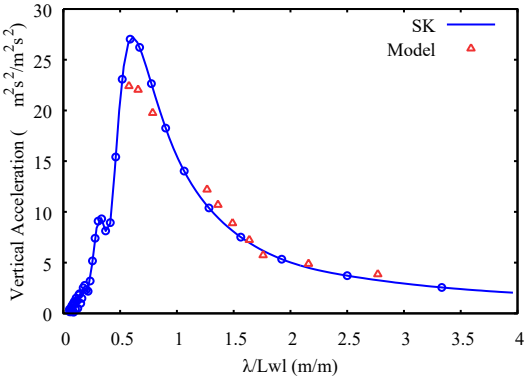

Figure 76. Point 4 – Vertical Acceleration, Speed: 10 kn (Fr=0.1), Heading: 135°

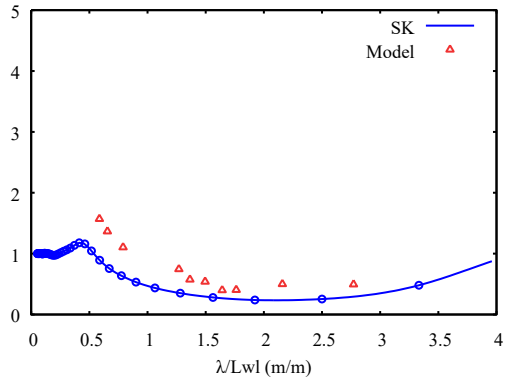

Figure 77. Point 6 – Relative Heave RAO, Speed: 10 kn (Fr=0.1), Heading: 135°

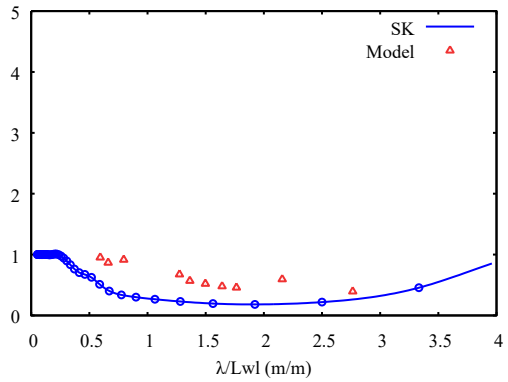

Figure 78. Point 8 – Relative Heave RAO, Speed: 10 kn (Fr=0.1), Heading: 135°

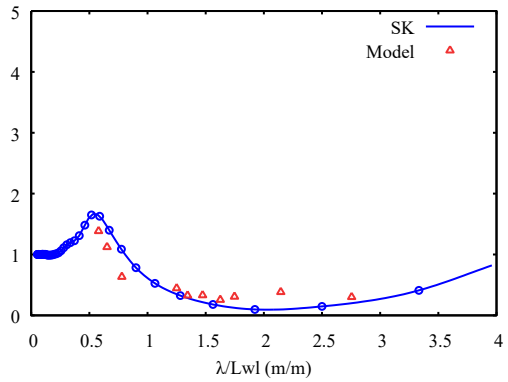

Figure 79. Point 10 – Relative Heave RAO, Speed: 10 kn (Fr=0.1), Heading: 135°

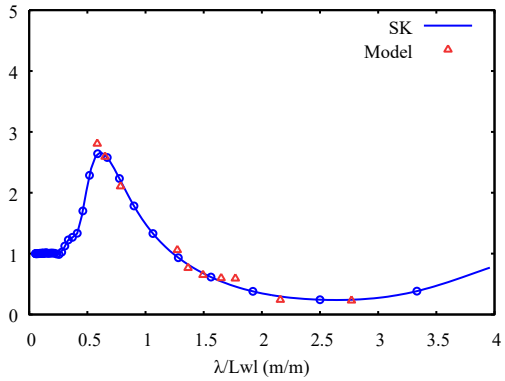

Figure 80. Point 12 – Relative Heave RAO, Speed: 10 kn (Fr=0.1), Heading: 135°

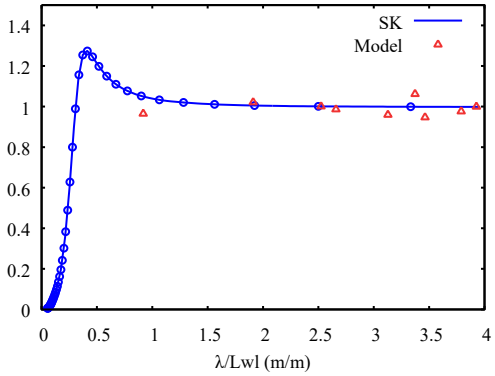

Figure 81. CG – Heave RAO, Speed: 10 kn (Fr=0.1), Heading: 90°

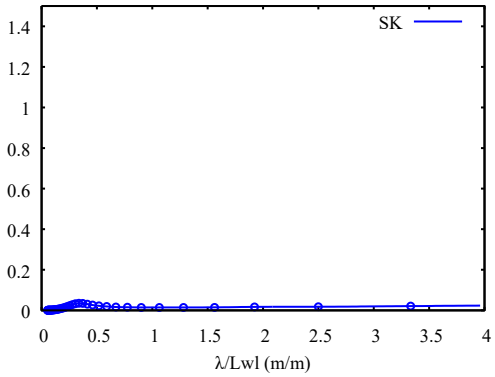

Figure 82. CG – Pitch RAO, Speed: 10 kn (Fr=0.1), Heading: 90°

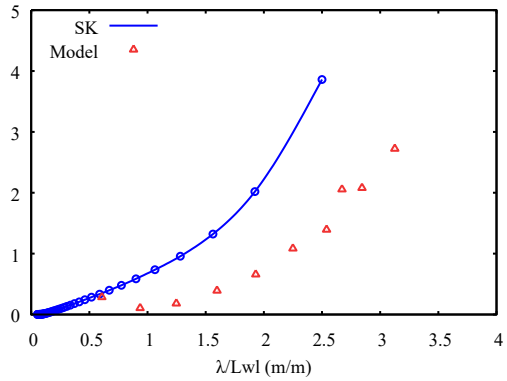

Figure 83. CG – Roll RAO, Speed: 10 kn (Fr=0.1), Heading: 90°

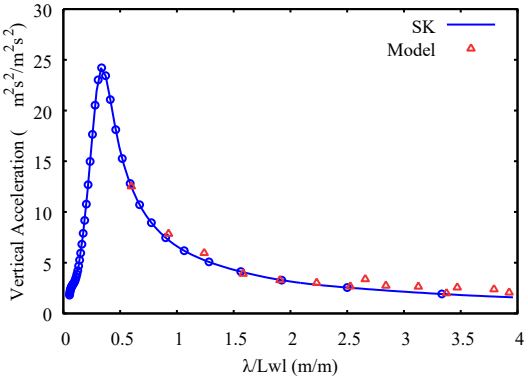

Figure 84. Point 4 – Vertical Acceleration, Speed: 10 kn (Fr=0.1), Heading: 90°

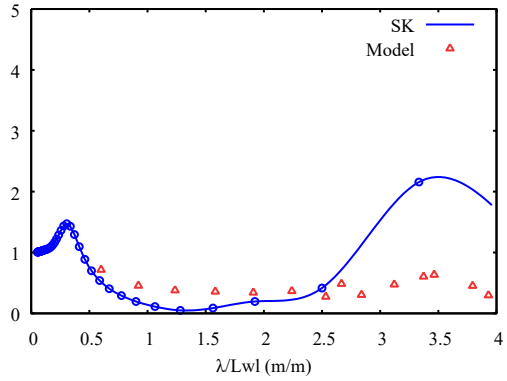

Figure 85. Point 6 – Relative Heave RAO, Speed: 10 kn (Fr=0.1), Heading: 90°

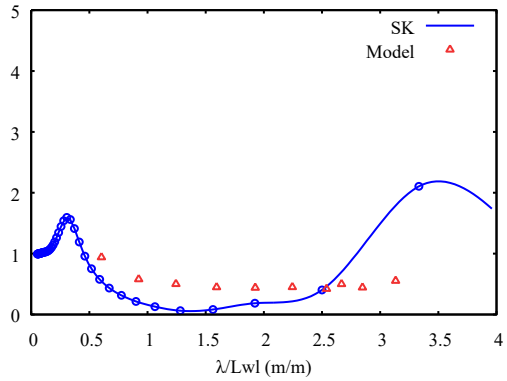

Figure 86. Point 8 – Relative Heave RAO, Speed: 10 kn (Fr=0.1), Heading: 90°

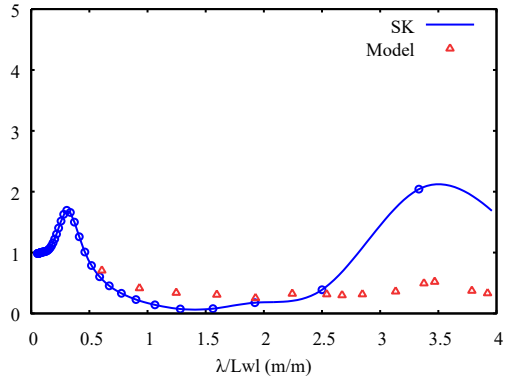

Figure 87. Point 10 – Relative Heave RAO, Speed: 10 kn (Fr=0.1), Heading: 90°

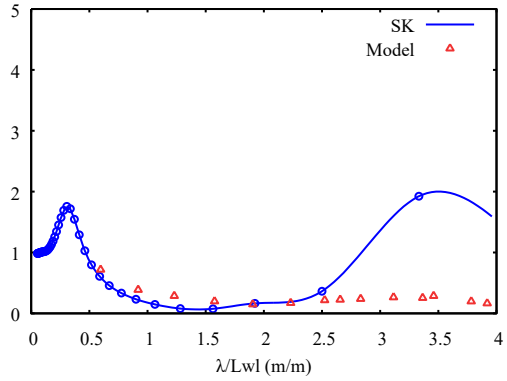

Figure 88. Point 12 – Relative Heave RAO, Speed: 10 kn (Fr=0.1), Heading: 90°

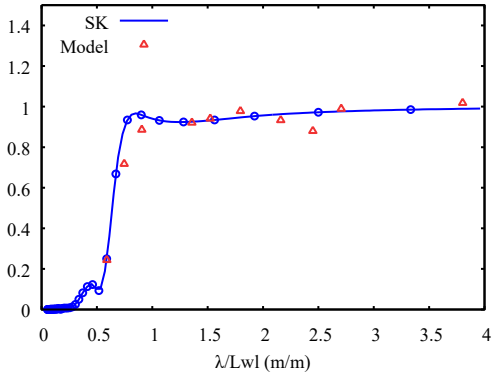

Figure 89. CG – Heave RAO, Speed: 22 kn (Fr=0.22), Heading: 135°

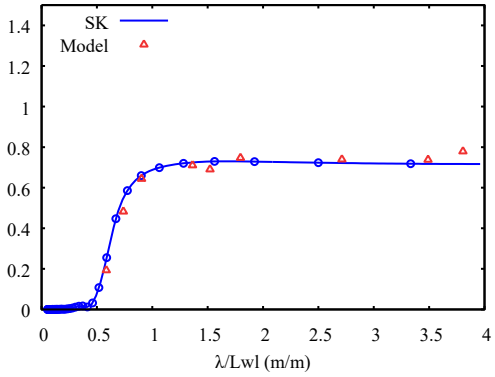

Figure 90. CG – Pitch RAO, Speed: 22 kn (Fr=0.22), Heading: 135°

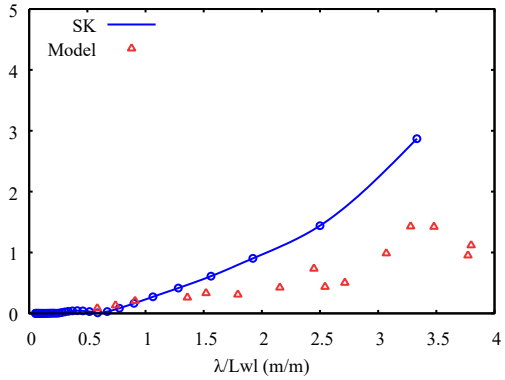

Figure 91. CG – Roll RAO, Speed: 22 kn (Fr=0.22), Heading: 135°

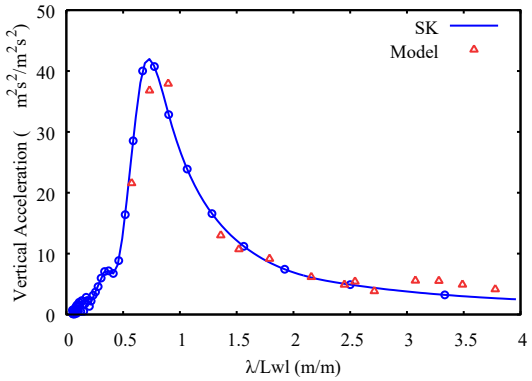

Figure 92. Point 4 – Vertical Acceleration, Speed: 22 kn (Fr=0.22), Heading: 135°

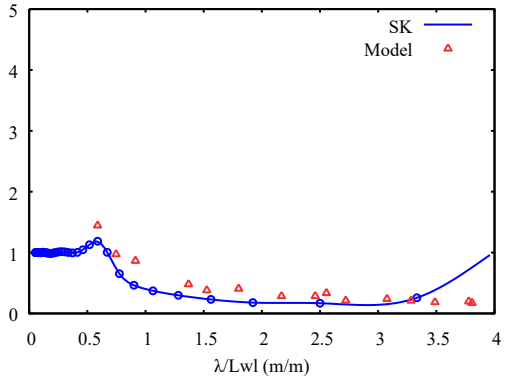

Figure 93. Point 6 – Relative Heave RAO, Speed: 22 kn (Fr=0.22), Heading: 135°

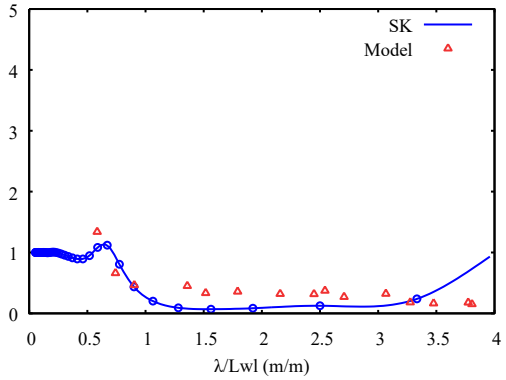

Figure 94. Point 8 – Relative Heave RAO, Speed: 22 kn (Fr=0.22), Heading: 135°

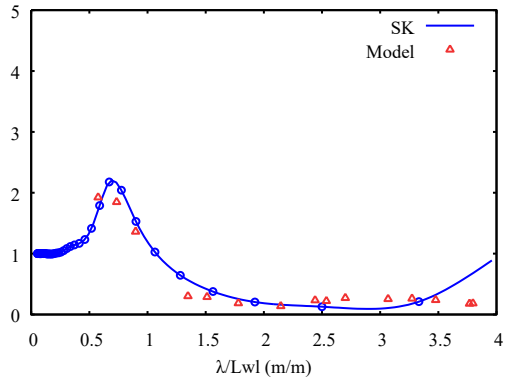

Figure 95. Point 10 – Relative Heave RAO, Speed: 22 kn (Fr=0.22), Heading: 135°

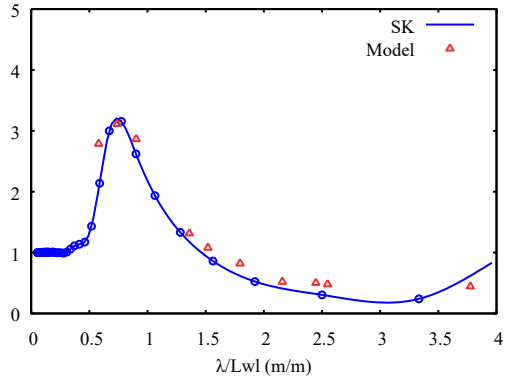

Figure 96. Point 12 – Relative Heave RAO, Speed: 22 kn (Fr=0.22), Heading: 135°

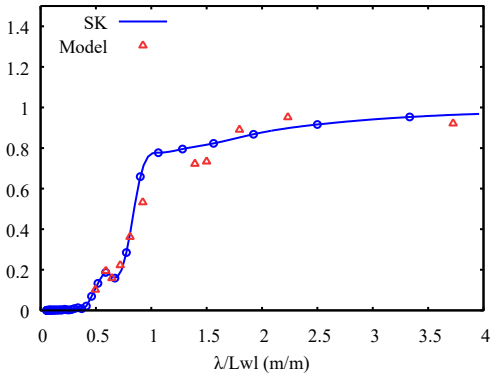

Figure 97. CG – Heave RAO, Speed: 22 kn (Fr=0.22), Heading: 180°

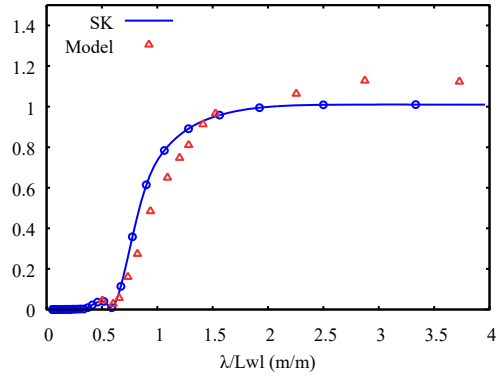

Figure 98. CG – Pitch RAO, Speed: 22 kn (Fr=0.22), Heading: 180°

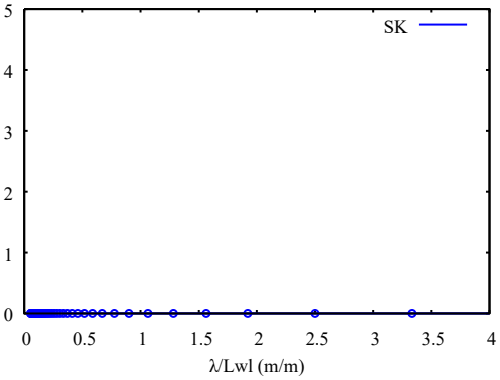

Figure 99. CG – Roll RAO, Speed: 22 kn (Fr=0.22), Heading: 180°

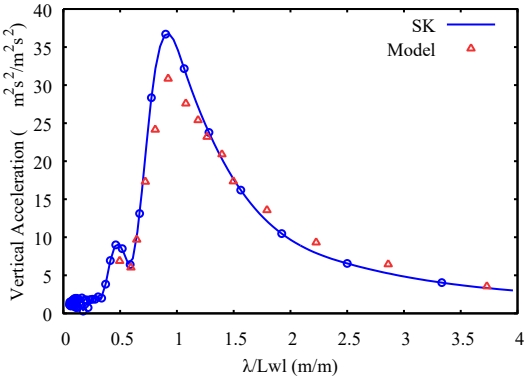

Figure 100. Point 4 – Vertical Acceleration, Speed: 22 kn (Fr=0.22), Heading: 180°

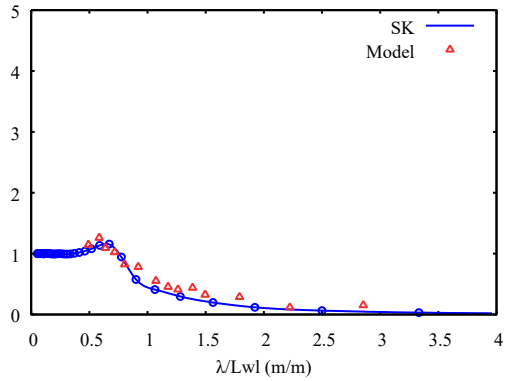

Figure 101. Point 6 – Relative Heave RAO, Speed: 22 kn (Fr=0.22), Heading: 180°

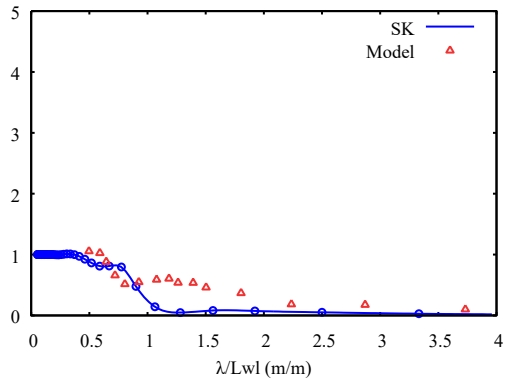

Figure 102. Point 8 – Relative Heave RAO, Speed: 22 kn (Fr=0.22), Heading: 180°

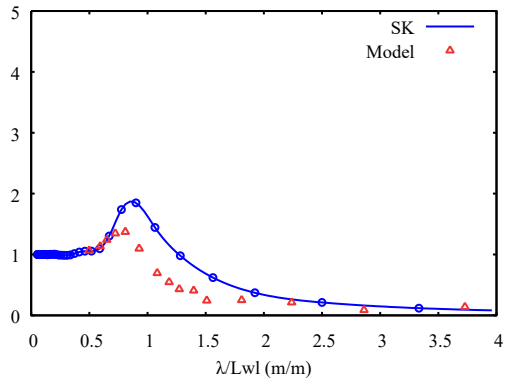

Figure 103. Point 10 – Relative Heave RAO, Speed: 22 kn (Fr=0.22), Heading: 180°

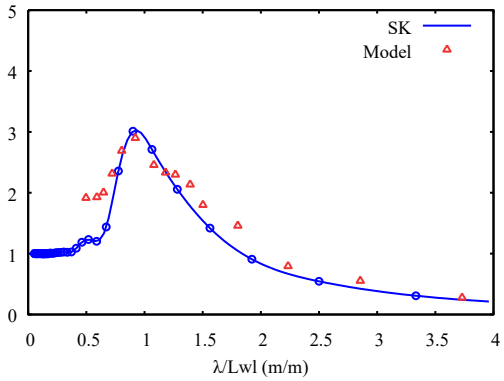

Figure 104. Point 12 – Relative Heave RAO, Speed: 22 kn (Fr=0.22), Heading: 180°

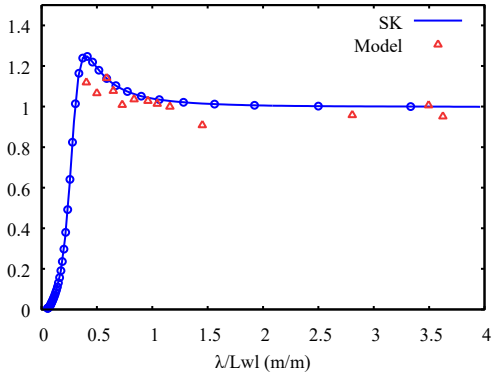

Figure 105. CG – Heave RAO, Speed: 22 kn (Fr=0.22), Heading: 90°

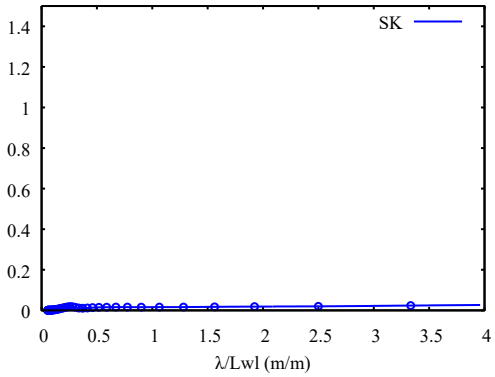

Figure 106. CG – Pitch RAO, Speed: 22 kn (Fr=0.22), Heading: 90°

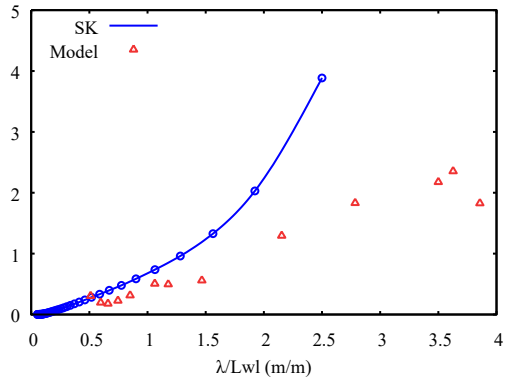

Figure 107. CG – Roll RAO, Speed: 22 kn (Fr=0.22), Heading: 90°

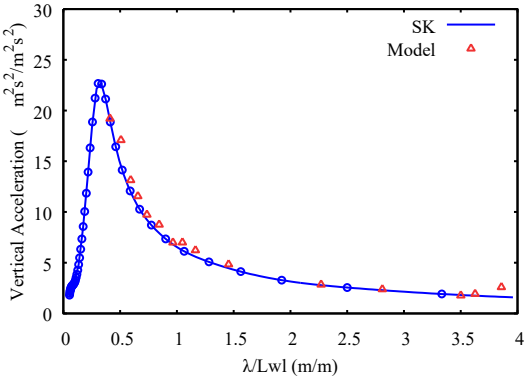

Figure 108. Point 4 – Vertical Acceleration, Speed: 22 kn (Fr=0.22), Heading: 90°

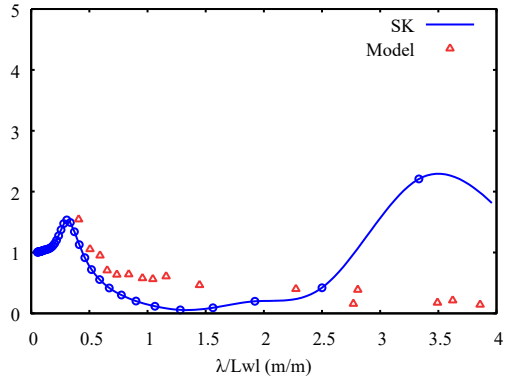

Figure 109. Point 6 – Relative Heave RAO, Speed: 22 kn (Fr=0.22), Heading: 90°

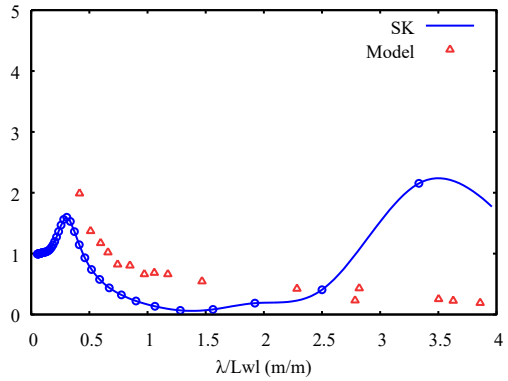

Figure 110. Point 8 – Relative Heave RAO, Speed: 22 kn (Fr=0.22), Heading: 90°

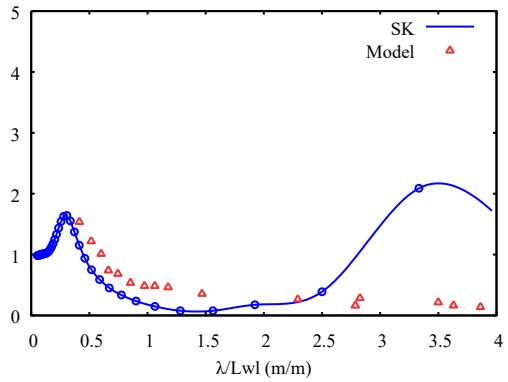

Figure 111. Point 10 – Relative Heave RAO, Speed: 22 kn (Fr=0.22), Heading: 90°

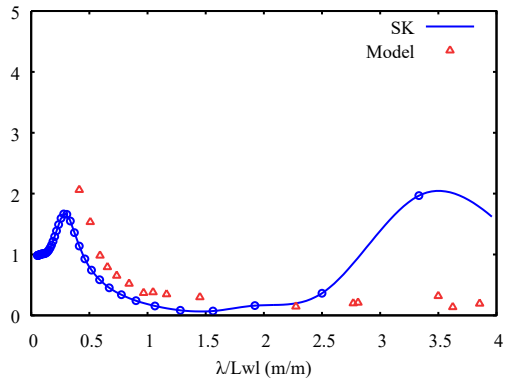

Figure 112. Point 12 – Relative Heave RAO, Speed: 22 kn (Fr=0.22), Heading: 90°

RAOs for KCS with Weight Distribution in Head Seas and Zero Speed

The heave and pitch RAOs for the full-scale KRISO Container Ship (KCS) hull geometry were computed in head seas and zero speed and compared to 1:100 scale model test data. An isometric view and body plan of the hull geometry file is given by Figure 113. The origin was placed amidships at 415.735 ft aft of the forward-most station. Table 4 also gives the dimensions and the loading condition as specified in GHS. The weight distribution used in the computations is shown by Figure 114. The pitch and yaw gyradii were computed automatically from the weight distribution and are given in Table 4. This distribution is the full-scale version of the experimental weight distribution of the model during testing.

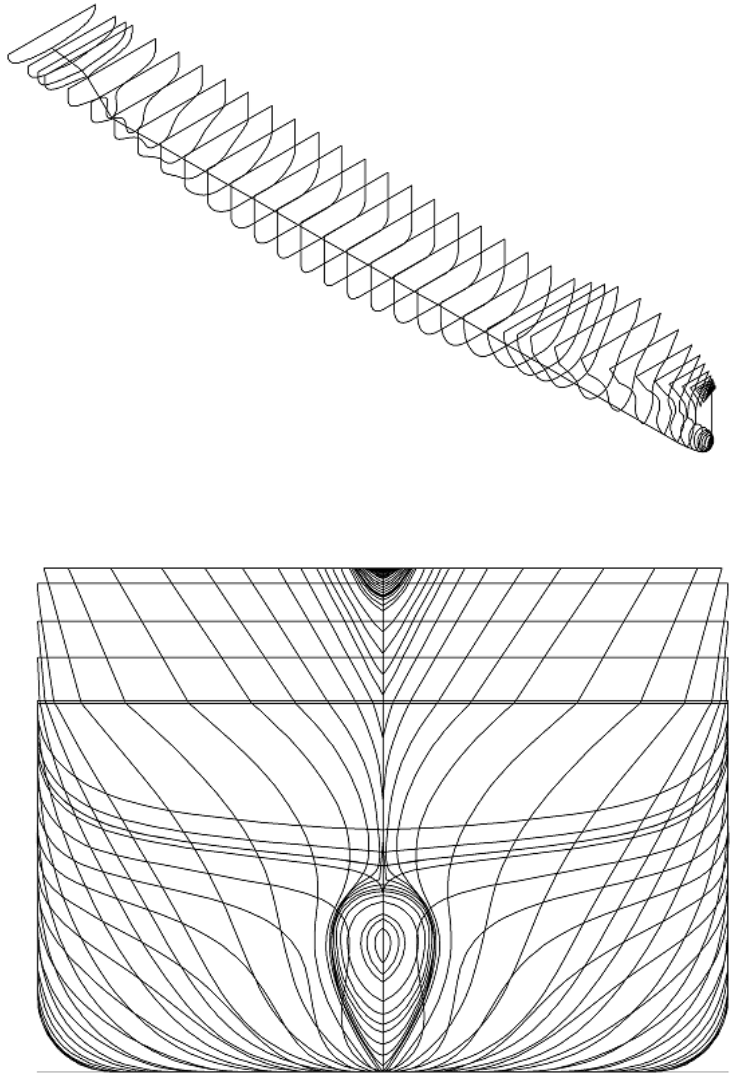

Figure 113. KCS Hull Geometry

L_{OA}	800.013	Ft	LCG	0.0	Ft, aft *0*
L_{WL}	783.94	Ft	TCG	0.0	Ft, *0*
B_{WL}	105.76	Ft	VCG	47.0	Ft, *0*
Δ	52,525.61	LT	LCF	32.94	Ft, aft *0*
C_B	0.592	-	GM_T	2.13	Ft
Draft	35.431	Ft	k_4	42.310	Ft
Trim	0.0	Deg, aft	k_5	202.226	Ft
Heel	0.0	Deg	k_6	202.226	Ft

Table 4. KRISO Container Ship Details

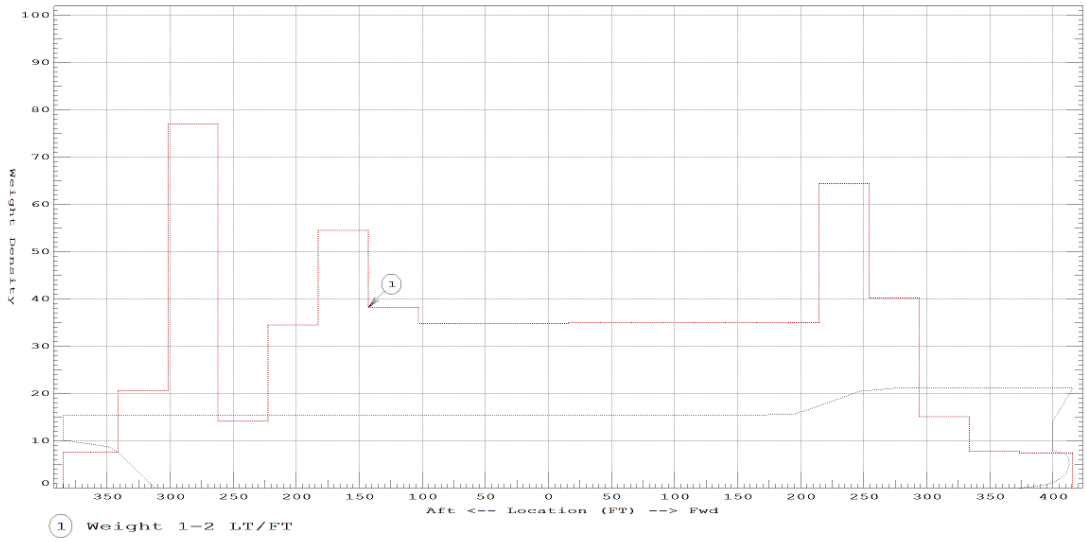

Figure 114. KCS Computational Full-Scale Weight Distribution

The experimental RAOs were measured at LBP/2 and on centerline. A GHS Critical Point was placed at this location, and the RAOs shown by Figure 115 were computed at this point. In general, the computational and experimental results are in good agreement.

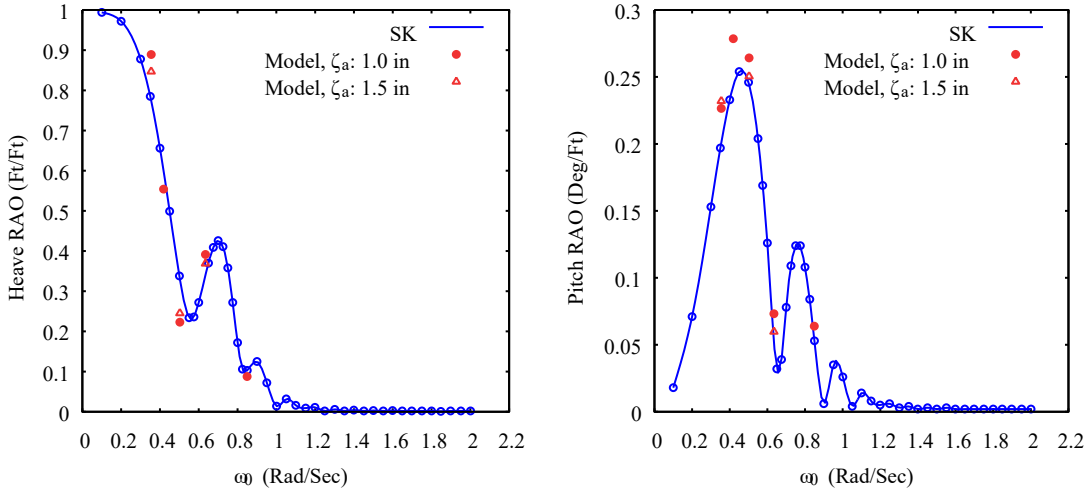

Figure 115. Heave and Pitch RAOs, Speed: 0 kn, Heading: 180°

References and Additional Resources

Journee, J. (2001). *Verification and Validation of Ship Motions Program SEAWAY*. Delft: Delft University of Technology Ship Hydromechanics Laboratory. Retrieved Jan. 11, 2018

Vugts, J. (1968). The Hydrodynamic Coefficients for Swaying, Heaving, and Rolling Cylinders in a Free Surface. *International Shipbuilding Progress, 15*. Retrieved Jan. 15, 2018, from http://mararchief.tudelft.nl/file/409/

Zhou, Z.-Q., Zhou, D.-C., & Xie, N. (1996). *A Seakeeping Experiment Research on Flokstra Container Ship Model.*